Title

Human TRMT1 and TRMT1L paralogs ensure the proper modification state, stability, and function of tRNAs.

Journal

Cell Reports, 44(1)

Authors

Zhang, Kejia

Manning, Aidan

Lentini, Jenna

et al.

Publication Date

2025-01-28

DOI

10.1016/j.celrep.2024.115092

Peer reviewed

HHS Public Access

Author manuscript

Cell Rep. Author manuscript; available in PMC 2025 February 17.

Published in final edited form as:

Cell Rep. 2025 January 28; 44(1): 115092. doi:10.1016/j.celrep.2024.115092.

Human TRMT1 and TRMT1L paralogs ensure the proper modification state, stability, and function of tRNAs

Kejia Zhang[1,6], **Aidan C. Manning**[2,6], **Jenna M. Lentini**[1], **Jonathan Howard**[2], **Felix Dalwigk**[3], **Reza Maroofian**[4], **Stephanie Efthymiou**[4], **Patricia Chan**[2], **Sergei I. Eliseev**[1], **Zi Yang**[1], **Hayley Chang**[1], **Ehsan Ghayoor Karimiani**[4], **Behnoosh Bakhshoodeh**[5], **Henry Houlden**[4,7], **Stefanie M. Kaiser**[3,7], **Todd M. Lowe**[2,7], **Dragony Fu**[1,7,8,*]

[1]Department of Biology, Center for RNA Biology, University of Rochester, Rochester, NY, USA

[2]Department of Biomolecular Engineering, University of California, Santa Cruz, Santa Cruz, CA, USA

[3]Institute of Pharmaceutical Chemistry, Goethe University Frankfurt, Max-von-Laue-Str. 9, 60438 Frankfurt, Germany

[4]Department of Neuromuscular Disorders, UCL Queen Square Institute of Neurology, WC1N 3BG London, UK

[5]Mashhad University of Medical Sciences, Mashhad, Razavi Khorasan Province 91778 99191, Iran

[6]These authors contributed equally

[7]Senior author

[8]Lead contact

SUMMARY

The tRNA methyltransferase 1 (TRMT1) enzyme catalyzes the *N2,N2*-dimethylguanosine (m2,2G) modification in tRNAs. Intriguingly, vertebrates encode an additional tRNA methyltransferase 1-like (TRMT1L) paralog. Here, we use a comprehensive tRNA sequencing approach to decipher targets of human TRMT1 and TRMT1L. We find that TRMT1 methylates all known tRNAs containing guanosine at position 26, while TRMT1L represents the elusive enzyme catalyzing m2,2G at position 27 in tyrosine tRNAs. Surprisingly, TRMT1L is also necessary for maintaining 3-(3-amino-3-carboxypropyl)uridine (acp3U) modifications in a subset of tRNAs

*Correspondence: dragonyfu@rochester.edu.

AUTHOR CONTRIBUTIONS

Conceptualization, K.Z., J.M.L., and D.F.; software, formal analysis, data curation, and visualization, A.C.M. and P.C.; investigation, K.Z., A.C.M., J.M.L., J.H., F.D., R.M., S.E., S.I.E., Z.Y., H.C., and E.G.K.; resources, S.E. and B.B.; writing – original draft, K.Z., A.C.M., and D.F.; writing – review & editing, K.Z., A.C.M., J.M.L., F.D., R.M., S.M.K., T.M.L., and D.F.; funding acquisition and supervision, H.H., S.M.K., T.M.L., and D.F.

DECLARATION OF INTERESTS

The authors declare no competing interests.

SUPPLEMENTAL INFORMATION

Supplemental information can be found online at https://doi.org/10.1016/j.celrep.2024.115092.

through a process that can be uncoupled from methyltransferase activity. We also demonstrate that tyrosine and serine tRNAs are dependent upon m2,2G modifications for their stability and function in translation. Notably, human patient cells with disease-associated TRMT1 variants exhibit reduced levels of tyrosine and serine tRNAs. These findings uncover unexpected roles for TRMT1 paralogs, decipher functions for m2,2G modifications, and pinpoint tRNAs dysregulated in human disorders caused by tRNA modification deficiency.

In brief

Zhang et al. elucidate the targets of a tRNA modification enzyme family and identify unanticipated roles for a duplicated tRNA modification enzyme that can be uncoupled from its ancestral function. These findings uncover the molecular mechanisms by which tRNAs are dysregulated in human disorders caused by tRNA modification deficiency.

Graphical Abstract

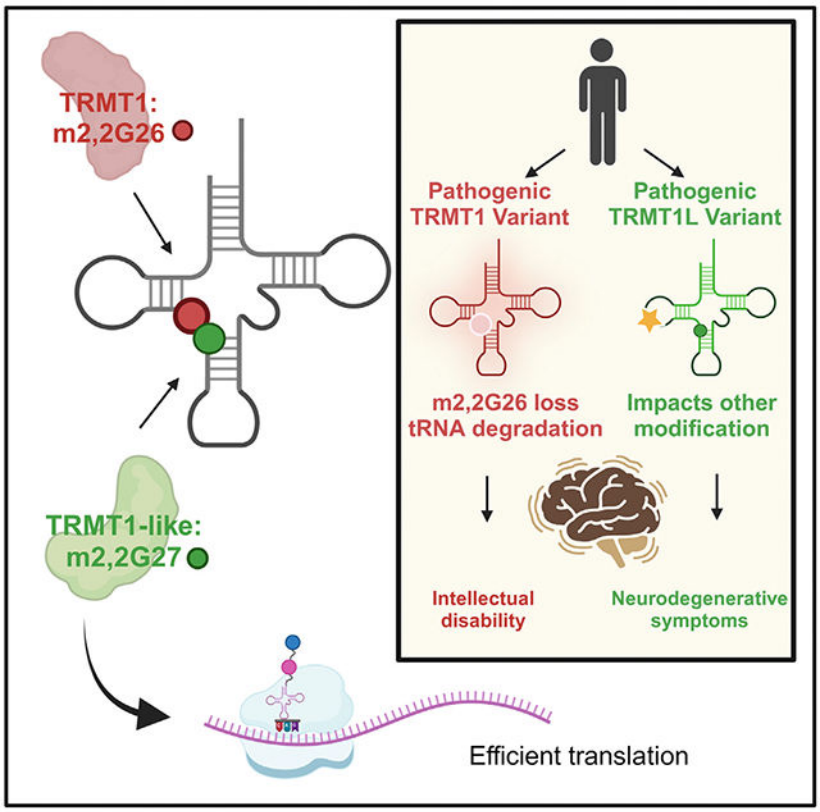

INTRODUCTION

Over 100 different types of post-transcriptional modifications have been identified in tRNAs.[1–3] Several of the modifications have been demonstrated to play critical roles in tRNA folding and biogenesis.[4] Moreover, tRNA modifications have emerged as key modulators of gene expression during organismal development, the cellular stress response, and tumorigenesis.[5–8] In particular, the brain appears to be sensitive to perturbations

in tRNA modification, as evidenced by the numerous cognitive disorders linked to tRNA modification enzymes.[9–11] While the connections between tRNA modification and biological pathways are growing, there are still major gaps in knowledge regarding the enzymes responsible for known and predicted tRNA modifications in humans.[12]

One of the first tRNA modification enzymes identified is tRNA methyltransferase 1 (Trm1p) from the yeast *Saccharomyces cerevisiae*.[13] Trm1p catalyzes the dimethylation of guanosine at position 26 in cytosolic and mitochondrial tRNAs to yield the *N*2,*N*2-dimethylguanosine (m2,2G) modification. Crystallographic and simulation studies have shown that the m2,2G modification plays a key role in preventing alternative tRNA conformations through destabilizing specific base-pairing interactions.[14–17] Consistent with this function, Trm1p-null strains in *S. cerevisiae* and *Schizosaccharomyces pombe* yeast exhibit defects in tRNA stability that are exacerbated in combination with deletion of either the Trm4p tRNA methyltransferase or the La RNA binding protein.[18–21]

In humans, the tRNA methyltransferase 1 (*TRMT1*) gene encodes a homolog of yeast Trm1p.[22,23] Like yeast Trm1p, human TRMT1 is required for the formation of m2,2G or *N*2-methylguanosine (m2G) in cytosolic and mitochondrial tRNAs.[24,25] Exome sequencing studies have identified pathogenic variants in *TRMT1* as the cause of certain forms of autosomal-recessive intellectual disability (ID) disorders.[26–31] Patient cells with biallelic ID-associated TRMT1 variants exhibit global deficits in m2,2G modification.[25,30,31] Consistent with loss of function, the ID-associated TRMT1 variants are defective in tRNA binding and enzymatic activity.[24,30,31] These studies highlight the critical role of TRMT1-catalyzed tRNA modification in ensuring proper development and cognitive function.

In addition to TRMT1, vertebrate genomes encode a TRMT1 paralog encoded by the tRNA methyltransferase 1-like (*TRMT1L*) gene.[24,25,32] Both TRMT1 and TRMT1L contain a class I *S*-adenosyl-methionine (SAM)-binding methyltransferase domain and zinc-finger motifs (Figure 1A), but methyltransferase activity has only been shown for human TRMT1.[23] In addition to the methyltransferase domain, TRMT1 contains a mitochondrial targeting signal at the amino terminus and nuclear localization sequence that are each required for TRMT1 localization to the mitochondria and nucleoplasm of human cells, respectively (Figure 1A).[24,25] In contrast to the nucleoplasmic and mitochondrial localization of TRMT1, TRMT1L is highly enriched in the nucleolus of human cells.[24,25]

Here, we applied a comprehensive tRNA sequencing approach to elucidate the human tRNA transcriptome modified by TRMT1 and TRMT1L. This approach has yielded a global overview of tRNA modifications and their dependence on TRMT1 and TRMT1L. Notably, these studies reveal molecular roles for TRMT1 and TRMT1L activity in tRNA stability and function that are crucial for proper neurodevelopment in humans.

RESULTS

Human cytosolic and mitochondrial tRNAs containing G at position 26 are targets of TRMT1

To elucidate the targets of TRMT1 and TRMT1L, we generated HEK293T cell lines deficient in TRMT1 or TRMT1L using exon deletion via CRISPR gene editing. The TRMT1 and TRMT1L knockout (KO) cell lines were compared to a parental control wild-type (WT) cell line. We confirmed deletion of the genomic regions in both alleles of the TRMT1- and TRMT1L-KO cell lines using sequencing (Data S1). Immunoblotting revealed nearly undetectable TRMT1 or TRMT1L protein in the TRMT1- or TRMT1L-KO cell lines, respectively (Figure 1B).

To monitor changes in the tRNA transcriptome caused by TRMT1 or TRMT1L, we performed ordered two-template relay sequencing (OTTR-seq), an RNA sequencing methodology based upon a modified retroelement reverse transcriptase.[33] Using the OTTR-seq approach in these cell lines, we generated full-length read coverage for 206 of the 258 total tRNAs in the high-confidence human tRNA set,[34] encompassing all 46 canonical tRNA isoacceptor families (Figures S1A–S1C).

We next leveraged modification-induced misincorporations in the data to reveal potential changes in base modifications. Initially, we validated that the misincorporations in our dataset were indicative of known base modifications based upon pre-treatment of samples with the *E. coli* AlkB demethylase, which can remove 1-methyladenosine (m1A), 3-methylcytosine (m3C), and 1-methylguanosine (m1G) modifications.[35,36] We observed a high percentage of misincorporation at position 58, indicative of the m1A modification that was abolished by AlkB treatment (Figure 1C, position 58:A). Moreover, we detected a misincorporation signature at position 26, indicative of the m2,2G modification that was reduced but not completely abolished after pre-treatment with AlkB (Figure 1C, position 26:G). These results are consistent with the known demethylase activity of AlkB on these different types of modifications.[37,38]

Investigation of misincorporations across all cytosolic tRNA transcripts in the control WT cells revealed additional sites of tRNA modification known to cause RT misincorporations, such as m1G at positions 9 and 37, 3-(3-amino-3-carboxypropyl)uridine (acp3U) at position 20, and m3C at position 32 (Figures 1D and S1D). In general, the modification profiles match those expected from previous studies in human cells.[36,39–42] Focusing on position 26, we identified misincorporations indicative of m2,2G or m2G in 132 of 234 cytosolic tRNAs (Figures 1D and S1D; Table S1). The misincorporation signature at position 26 for tRNA-Val and tRNA-iMet was distinct from other tRNAs, consistent with the presence of m2G instead of m2,2G in these tRNAs (STAR Methods). Notably, we observed loss of misincorporations at position 26 in cytosolic tRNAs of TRMT1-KO cells but not TRMT1L-KO cells (Figures 1D and S2A–S2C).

In addition to cytosolic tRNAs, we detected a misincorporation signature for m2G or m2,2G modification at position 26 in 5 of 22 mitochondrial (mt) tRNAs from control WT cells (Figure S3A; Table S2). The misincorporation signature at position 26 in the

mitochondrial tRNAs was abolished in TRMT1-KO cells but still present in the TRMT1L-KO cell line (Figures S3B and S3C). While m2G or m2,2G modification at position 26 has been identified in a subset of human mitochondrial tRNAs,[43] the cellular requirement for TRMT1 in the modification of mt-tRNA-Glu or mt-tRNA-Asn has not been tested. Using a primer extension assay in which the presence of m2G leads to an RT pause,[44,45] we found that the m2G modification at position 26 in mt-tRNA-Asn and mt-tRNA-Glu was reduced to background levels in the TRMT1-KO cell lines but retained in the TRMT1L-KO cell line (Figures S3D and S3E). Altogether, these studies demonstrate that TRMT1 is the primary enzyme responsible for all detectable m2G or m2,2G modifications at position 26 in nucleus- and mitochondrion-encoded tRNAs.

TRMT1 and TRMT1L are required for distinct m2,2G modifications in tyrosine tRNAs

In contrast to TRMT1, no enzymatic activity has been described for its paralog TRMT1L. As noted above, the misincorporation frequency at position G26 in tRNAs was abolished in TRMT1-KO cells but not significantly impacted in TRMT1L-KO cell lines (Figures 2A, and S2C). Interestingly though, we observed a reduction in misincorporation frequency at position 27 in tRNA-Tyr isodecoders of the TRMT1L-KO strain but not TRMT1-KO cells (Figures 2A and S2D). Consistent with the reduction in modification at position 27 of tRNA-Tyr, we observed an increase in read coverage for mature tRNA-Tyr-GUA in the TRMT1L-KO cell line, caused by increased readthrough by the RT (Figure S2E). Unlike all other human tRNAs, the tRNA-Tyr family exhibits the unique property of containing two consecutive m2,2G modifications at positions 26 and 27 (Figure 2B).[46–48] These data suggest that TRMT1 modifies position 26 in tRNA-Tyr, while TRMT1L represents the enzyme that modifies position 27 in tRNA-Tyr.

To investigate the role of TRMT1 and TRMT1L in the modification of tRNA-Tyr, we generated a TRMT1-TRMT1L double KO (DKO) cell line to ascertain whether there was redundancy in either of the modification enzymes. The DKO cell line was generated in a similar manner as above by removing exon 1 of the TRMT1L gene in the TRMT1-KO cell line described above. Immunoblotting revealed the absence of detectable TRMT1L protein in both the TRMT1L-KO and DKO cell lines compared to the control WT cell line (Figure 2C).

To directly test the presence of m2,2G modifications, we isolated tyrosine tRNA isoacceptors using biotin oligonucleotides followed by nucleoside analysis via liquid chromatography-mass spectrometry (LC-MS). We find that tyrosine tRNAs from TRMT1-KO cells contain ~50% of the m2,2G modification compared to control WT cell lines (Figure 2D, TRMT1-KO). Tyrosine tRNAs from TRMT1L-KO cells also contain ~50% of the m2,2G modification compared to control WT cell lines (Figure 2D, TRMT1L-KO). The reduction in m2,2G modification by approximately half in the TRMT1-KO or TRMT1L-KO cell lines is consistent with each enzyme being responsible for one m2,2G modification in tRNA-Tyr. Furthermore, we find that m2,2G modification in tyrosine tRNAs is reduced to near background levels in the TRMT1-TRMT1L DKO cell line (Figure 2D, T1T1L-DKO). In addition to m2,2G modifications, we found that the acp3U modification in tRNA-Tyr was decreased in the TRMT1L and DKO cell lines (Figure 2D, acp3U).

We independently confirmed the changes in tRNA-Tyr modification state in TRMT1-KO, TRMT1L-KO, and DKO cell lines using absolute quantification via MS coupled to stable isotope-labeled internal standards (SILIS).[49,50] Using this approach, we detected two m2,2G modifications per tRNA-Tyr molecule from control WT human cells (Figure S4A). Consistent with results above, the amount of m2,2G in tRNA-Tyr decreased to approximately one m2,2G per tRNA-Tyr from the TRMT1-KO or TRMT1L-KO cell lines and decreased to near background levels in the DKO cell line (Figure S4A).

To validate that TRMT1 and TRMT1L are required for methylating positions 26 and 27, respectively, we developed a primer extension assay to resolve the consecutive m2,2G modifications in tRNA-Tyr isoacceptors at single-nucleotide resolution. Using this assay, we could detect a stop at position 27 with minimal readthrough products in control WT cells, while a control reaction without RT yielded no detectable stop at position 27 (Figure 2E, lanes 1 and 2; see Figures S5A and S5B for the sequencing ladder). In the TRMT1-KO cell line, the stop at position 27 was still detectable, consistent with TRMT1L modification (Figure 2E, lane 3). We note that a slight readthrough product could be detected in the TRMT1-KO cell line, indicating that position 26 was affected. In the TRMT1L-KO cell line, the RT block at position 27 was greatly diminished with the appearance of an RT block 1 nt upstream at position 26 (Figure 2E, lane 4). Notably, the block at position 26 was abolished in the DKO cell line with readthrough products up to the acp3U modification at position 20 and m2G modifications at positions 9 and 6 (Figures 2E, lane 5, and S5B). These results are consistent with TRMT1 and TRMT1L methylating positions 26 and 27, respectively, in tRNA-Tyr isoacceptors.

To confirm the role of TRMT1L in formation of m2,2G at position 27 in tRNA-Tyr, we performed rescue experiments via re-expression of WT or mutant versions of TRMT1L in the TRMT1L-KO cell line. We created a construct that expresses a TRMT1L mutant in which the predicted aspartic acid residue that binds SAM in the methyltransferase catalytic site was changed to alanine (TRMT1L-D373A). We generated TRMT1L-KO cell lines with empty vector or constructs expressing WT TRMT1L or the TRMT1L-D373A mutant (Figure 2F). As shown above, tRNA-Tyr from control WT cells exhibited a primer extension stop at position 27 that was not detected without RT (Figure 2G, lanes 1 and 2). Confirming our results above, the TRMT1L-KO cell lines with vector alone exhibited background levels of m2,2G stop at position 27 in tRNA-Tyr compared to WT control cells (Figure 2G, lane 3). Re-expression of WT TRMT1L in TRMT1L-KO cells was sufficient to restore m2,2G formation at position 27 in tRNA-Tyr (Figure 2G, lane 4). Only background levels of m2,2G were detected at position 27 upon re-expression of the TRMT1L variant with a catalytic site mutation in the TRMT1L-KO cell line (Figure 2G, lane 5).

As further validation of a role of TRMT1L in tyrosine tRNA modification, we employed the Positive Hybridization in the Absence of modification (PHA) assay.[51,52] This northern blot-based assay relies on differential probe hybridization to tRNA caused by the presence or absence of m2,2G, which impairs base-pairing. Thus, a decrease in m2,2G modification leads to an increase in PHA probe signal. Using this approach, we detected an increase in PHA probe signal for tRNA-Tyr-GUA in the TRMT1L-KO cell line compared to control WT cells (Figures 2H and 2I). The increased PHA probe hybridization for tRNA-Tyr in

TRMT1L-KO cells is consistent with loss of m2,2G at position 27 in tyrosine tRNAs. Re-expression of WT-TRMT1L in the TRMT1L-KO cell lines reduced the PHA signal back to WT levels compared to TRMT1L-KO cells with vector (Figures 2H and 2I, WT). In contrast, expression of the TRMT1L-D373A mutant had no major change in the PHA signal of tRNA-Tyr-GUA in the TRMT1L-KO cell line compared to vector alone (Figures 2H and 2I, D373A). Altogether, these results indicate that TRMT1 and TRMT1L are required for the m2,2G modification at positions 26 and 27, respectively, in tyrosine tRNAs.

TRMT1 and TRMT1L catalyze m2,2G formation at specific positions in tRNA-Tyr

While tRNA methyltransferase activity has been demonstrated for human TRMT1,[23] the enzymatic activity of TRMT1L remains to be shown, and it remains possible that TRMT1L plays an indirect role in generating m2,2G in tRNA-Tyr. Thus, we tested the methyltransferase activity of purified TRMT1 or TRMT1L on *in vitro*-transcribed tRNA-Tyr substrates. TRMT1 or TRMT1L fused to the tandem Strep tag were expressed and purified from human cells using the Strep tag purification system (Figure 3A). No m2,2G or m2G modification was detected in tRNA-Tyr after pre-incubation with buffer from a mock control purification (Figure 3B). In contrast, pre-incubation of tRNA-Tyr with purified TRMT1 or TRMT1L revealed the formation of m2,2G as well as m2G (Figure 3B).

We next verified that the *in vitro* activity of TRMT1 and TRMT1L was specific to positions 26 and 27 of tRNA-Tyr, respectively, using the primer extension assay. No extension product was detected with tRNA-Tyr in the absence of RT (Figure 3C, lane 1). Primer extension with tRNA-Tyr pre-incubated with buffer led to the generation of full-length product with only background signal at positions 26 and 27 (Figure 3C, lane 6). Pre-incubation of tRNA-Tyr with purified TRMT1, followed by primer extension, revealed the appearance of an RT block indicative of m2,2G formation at position 26, but not position 27 (Figure 3C, lane 7; quantified in Figure 3D). The tRNA-Tyr incubated with TRMT1L exhibited a predominant RT stop at position 27 (Figure 3C, lane 8; quantified in Figure 3D). Thus, purified TRMT1 and TRMT1L can catalyze m2,2G formation in tRNA-Tyr at positions 26 and 27, respectively.

Since all human tRNA-Tyr genes contain an intron, we also tested the activity of TRMT1 and TRMT1L on *in vitro*-transcribed pre-tRNA-Tyr substrates with an intron. No extension product was detected in the absence of RT (Figure 3E, lane 1). Primer extension with pre-tRNA-Tyr incubated with buffer led to the generation of full-length product with only background signal at positions 26 and 27 (Figure 3E, lane 6). An RT block was detected at position 26 in pre-tRNA-Tyr after incubation with TRMT1 (Figure 3E, lane 7; quantified in Figure 3D). In contrast, no RT block was detected at either position 26 or 27 in pre-tRNA-Tyr after incubation with TRMT1L (Figure 3E, lane 8; quantified in Figure 3D). These results show that TRMT1 can catalyze m2,2G formation in mature as well as pre-tRNA-Tyr substrates containing an intron, while TRMT1L exhibits detectable activity only on mature tRNA-Tyr.

In addition to WT tRNA-Tyr substrates, we tested the activity of TRMT1 and TRMT1L on tRNA-Tyr substrates in which G26 or G27 was mutated to A (G26A or G27A). Replicating our results above, pre-incubation of WT tRNA-Tyr-GAU containing G26 and G27 with

purified TRMT1 or TRMT1L, followed by primer extension, revealed the appearance of an RT block indicative of m2,2G formation at positions 26 or 27, respectively (Figure 3F, lanes 3 and 4). Intriguingly, we could detect a minor stop signal at position 27 instead of 26 with the tRNA-Tyr G26A variant after incubation with TRMT1 (Figure 3F, lane 6; quantified in Figure 3D). We could still detect the formation of m2,2G at position 27 for the tRNA-Tyr G26A variant incubated with TRMT1L (Figure 3F, lane 7; quantified in Figure 3D). The formation of m2G and m2,2G in tRNA-Tyr G26A by TRMT1 or TRMT1L was confirmed by LC-MS (Figures S6A and S6B). These results suggest that TRMT1L can modify G27 independent of the nucleotide status at position 26, while TRMT1 can modify G at position 27 to a minor extent when the preceding nucleotide position is no longer G.

For the tRNA-Tyr G27A variant, we could detect an RT block at position 26 after incubation with TRMT1 (Figure 3G, lane 9; quantified in Figure 3D). In contrast, no RT block above background was detected at position 26 or 27 of tRNA-Tyr G27A after incubation with TRMT1L (Figure 3G, lane 10; quantified in Figure 3D). LC-MS analysis validated the formation of m2,2G in tRNA-Tyr G27A by TRMT1 but not TRMT1L (Figures S6A and S6B). This result indicates that TRMT1L has specificity for G at position 27 and does not switch to modifying position 26 if position 27 is no longer a modification target. Moreover, the retention of TRMT1 activity on tRNA-Tyr G27A is consistent with prior work showing that the two base pairs preceding G26 in the D stem are a prerequisite for recognition by TRMT1 homologs, while the identity of nucleotides downstream of G26 can vary among TRMT1 targets.[53]

As another test for the specificity of the enzymes, we tested the activity of TRMT1 and TRMT1L on an *in vitro*-transcribed tRNA-Ile-AAU, which contains m2,2G at position 26. Incubation of tRNA-Ile-AAU with TRMT1, but not TRMT1L, led to the formation of an RT block at position 26, indicative of m2,2G formation (Figure 3G, lanes 2 and 3; quantified in Figure 3D). In addition, we tested whether mutation of the A at position 27 of tRNA-Ile-UAU to G could convert tRNA-Ile-AAU to a TRMT1L substrate. While an RT block at position 26 was detected in tRNA-Ile A27G after incubation with TRMT1, only background signal was detected at positions 26 or 27 after incubation with TRMT1L (Figure 3G, lanes 5 and 6; quantified in Figure 3D). These results suggest that TRMT1L recognizes elements distinct to tRNA-Tyr in order to methylate position 27.

TRMT1 or TRMT1L deficiency impacts acp3U modification status in a distinct subset of tRNAs

In addition to m2,2G modification at position 26 and 27, we compared the misincorporation frequency at all other positions across the tRNA transcriptome between WT, TRMT1-KO, and TRMT1L-KO cell lines. A change in misincorporation frequency was detected at position 20 of tRNA-Ala isodecoders, which was reduced in the TRMT1-KO cell lines compared to control WT cells (Figure 4A, Ala). As shown above, tRNA-Ala contains m2,2G at position 26 catalyzed by TRMT1. Surprisingly, we also found that TRMT1L-KO cell lines exhibited a reduction in misincorporation at position 20 in tRNA-Ala as well as tRNA-Cys even though neither of these tRNAs contain m2,2G modification formed by TRMT1L (Figure 4A, Ala and Cys). Most tRNAs contain dihydrouridine at position 20 in the D

loop. However, dihydrouridine does not lead to modification-induced misincorporations using this methodology, based on our observations as well as previous findings.[36] Instead, the misincorporation pattern is consistent with the acp3U modification that is known to be present in human tRNA-Tyr, -Ala, -Cys, -Asn, and -Ile isoacceptors.[40,54,55] In human cells, the DTWD1 enzyme catalyzes the majority of acp3U modification in tRNA-Cys and tRNA-Tyr, while the DTWD2 enzyme catalyzes the formation of acp3U in tRNA-Asn and tRNA-Ile isoacceptors.[55] The D loop of tRNA-Ala isoacceptors matches the D loop in tRNA-Cys and tRNA-Tyr that is thought to be the recognition sequence of DTWD1.

We next used LC-MS analysis of purified tRNA-Ala, tRNA-Cys, tRNA-Asn, and tRNA-Ile to directly measure changes in acp3U modification. Consistent with the decrease in misincorporation frequency at position 20 of tRNA-Ala, we found that the acp3U modification was reduced in tRNA-Ala isoacceptors purified from the TRMT1-KO, TRMT1L-KO, and DKO cell lines (Figure 4B, tRNA-Ala). Also consistent with the tRNA sequencing data, the level of acp3U modification in tRNA-Cys was decreased in the TRMT1L-KO and DKO cell lines but not the TRMT1-KO cell line (Figure 4B, tRNA-Cys). We further validated the decrease in acp3U modification of tRNA-Ala and tRNA-Cys in the TRMT1-KO, TRMT1L-KO, and DKO cell lines using absolute quantification with SILIS (Figures S4B and S4C). In contrast to tRNA-Ala and tRNA-Cys, the TRMT1L-KO cell line exhibited an increase in acp3U modification in tRNA-Asn and tRNA-Ile (Figures 4B, tRNA-Asn and tRNA-Ile, and S6C–S6F). These findings suggest that TRMT1 and TRMT1L play a role in modulating acp3U modification at position 20 in the D loop of tRNAs.

To further confirm the changes in acp3U modification, we employed a primer extension assay, since acp3U is known to block primer extension by RTs.[56,57] Since tRNA-Cys does not contain m2,2G at position 26 that would inhibit primer annealing, this allowed us to design a primer hybridizing downstream of position 20 to monitor acp3U status (Figure 4C). Using this approach, we detected an RT block at position 20 in tRNA-Cys, indicative of the acp3U modification in the control WT cell line (Figure 4D, lane 1). The RT block at position 20 was greatly reduced in the TRMT1L-KO and DKO cell lines, leading to readthrough to an immediately upstream block or the end of the tRNA (Figure 4D, lanes 3 and 4; quantified in Figure 4E). The cause of the RT block at the upstream G is currently unknown but could be due to aberrant modification or structure of tRNA-Cys when lacking acp3U. The RT block at position 20 in tRNA-Cys was not greatly affected in the TRMT1-KO cell line (Figures 4D, lane 2, and 4E). These results confirm that the acp3U modification at position 20 in tRNA-Cys is affected by loss of TRMT1L expression but not TRMT1.

Identification of a TRMT1L variant that reduces acp3U but not m2,2G modification in tRNAs

In collaboration with clinicians matched through the GeneMatcher database,[58] we identified non-identical sibling patients homozygous for a rare TRMT1L variant who exhibited a range of early-onset neurodegenerative symptoms (Figure S7A, patients V.4 and V.5). These symptoms included distal motor neuropathy, leukodystrophy, ID, generalized hypotonia, and contractures. The proband has a homozygous missense variant in TRMT1L (NM_030934.5): c.1535C>T, p.(Pro512Leu). The variant segregates with the disease in the family and is

predicted to be deleterious based upon multiple pathogenicity prediction algorithms (Figures S7B and S7C). The P512 residue lies within the methyltransferase domain and is conserved among TRMT1L homologs (Figure 4F).

To investigate the functional impact of this missense variant, fibroblast cells were derived from a skin biopsy taken from the brother (hereafter referred to as P512L patient fibroblast cells). The TRMT1L-P512L patient fibroblast cells were compared to a control fibroblast cell line obtained from a healthy, age-matched individual with WT TRMT1L alleles. Using LC-MS, no major change in m2,2G or acp3U levels was detected in purified tRNA-Tyr from the TRMT1L-P512L patient fibroblast cells compared to the control fibroblast cell line (Figure 4G, tRNA-Tyr). In contrast, we detected a decrease in acp3U modification in tRNA-Ala and Cys isolated from the TRMT1L-P512L patient fibroblast cells (Figure 4G). These results suggest that the TRMT1L-P512L variant impairs acp3U modification in tRNA-Ala and Cys without a detectable impact on the m2,2G or acp3U modification in tRNA-Tyr.

We further confirmed and defined the molecular effect of the TRMT1L-P512L variant using our HEK293T cell line deficient in TRMT1L. As shown above, we had generated TRMT1L-KO cell lines containing integrated lentiviral vectors expressing either GFP alone, TRMT1L-WT, or the TRMT1L-D373A mutant that exhibits defects in rescuing m2,2G formation in tRNA-Tyr (Figure 2F). Using this same strategy, we generated a TRMT1L-KO cell line stably expressing the TRMT1L-P512L variant (Figure S7D). As described above, tRNA-Tyr from control WT cells exhibited a primer extension stop at position 27, while the TRMT1L-KO cell lines with vector alone exhibited background levels of m2,2G stop at position 27 in tRNA-Tyr (Figure 4H, lanes 2 and 3). Re-expression of WT TRMT1L, but not TRMT1L-D373A, in TRMT1L-KO cells was able to restore m2,2G formation at position 27 in tRNA-Tyr (Figure 4H, lanes 4 and 5). Consistent with the results in P512L patient fibroblast cells, the re-expression of TRMT1L-P512L in TRMT1L-KO cells was able to restore m2,2G formation at position 27 in tRNA-Tyr (Figure 4H, lane 6).

As shown above, tRNA-Cys from control-WT cells exhibited an RT block at position 20 of tRNA-Cys that was reduced in the TRMT1L-KO cell line with concomitant readthrough to the upstream nucleotide position (Figure 4I, lanes 2 and 3). Expression of WT TRMT1L rescued the RT block at position 20 (Figure 4I, lane 4). Notably, we find that expression of the TRMT1L-D373A mutant is able to rescue acp3U formation in tRNA-Cys despite being impaired in m2,2G formation in tRNA-Tyr (Figure 4I, lane 5). Consistent with the results in P512L patient fibroblast cells, expression of the TRMT1L-P512L variant exhibited only partial rescue of acp3U modification at position 20 in tRNA-Cys of TRMT1L-KO cells (Figure 4I, lane 6). Altogether, these findings uncover a variant in TRMT1L that impacts acp3U modification and show that TRMT1L function in m2,2G modification can be uncoupled from TRMT1L's effect on acp3U modification.

TRMT1-catalyzed modifications impact the levels of tRNA-Tyr and tRNA-Ser in human cells

We next investigated how loss of TRMT1 or TRMT1L affects the abundance of individual tRNAs using the OTTR-seq data. As noted above, we observed an increased read coverage for full-length mature tRNA-Tyr-GUA in the TRMT1L-KO cell line caused by increased

readthrough by the RT due to loss of m2,2G modification at position 27 of tRNA-Tyr (Figure S2E). In contrast to tRNA-Tyr, no other tRNAs exhibited a significant change in levels in the TRMT1L-KO cell line (Figure S2E).

An increase in full-length read abundance was observed for most G26-containing tRNAs in the TRMT1-KO cell line compared to the control-WT cell line (Figure 5A, red triangles). The increase in read abundance for G26-containing tRNAs in the TRMT1-KO cell line compared to the control-WT cell line is consistent with the lack of m2,2G modification at position 26 in the TRMT1-KO cell line that allows for enhanced RT processivity and more full-length tRNA reads. The apparent increase in full-length tRNA reads in the TRMT1-KO cell line is further amplified by the incomplete removal of the m2,2G modification by AlkB in the WT control samples that leads to reduced levels of full-length tRNA reads relative to the TRMT1-KO samples.

However, in contrast to most G26-containing tRNAs, we found that all tRNA-Tyr isodecoders and a subset of tRNA-Ser isodecoders exhibited a decrease in abundance in the TRMT1-KO cell line (Figure 5A, blue triangles). Both tRNA-Tyr and tRNA-Ser isoacceptors contain m2,2G modifications at position 26 that are abolished in the TRMT1-KO cell line. We also measured tRNA modifications in purified tRNA-Ser isoacceptors and detected only background levels of m2,2G in tRNA-Ser purified from TRMT1-KO cells (Figure S6G). Interestingly, we also found that the m3C, Um, and i6A modifications are reduced in tRNA-Ser isolated from TRMT1-KO cells (Figure S6G). These results suggest a role for TRMT1 in the cellular accumulation of tRNA-Tyr and tRNA-Ser isodecoders as well as maintaining the normal modification patterns present in these tRNAs.

To confirm these findings, we performed northern blotting using probes against tRNA-Tyr and tRNA-Ser. Consistent with the sequencing data, we find that tRNA-Tyr-GUA isoacceptors exhibited an ~50% decrease in the TRMT1-KO and TRMT1-TRMT1L-DKO cell lines but not in the TRMT1L-KO cell line (Figures 5B and 5C). TRMT1-KO and DKO cells also exhibited an ~50% percent decrease in tRNA-Ser-GCU (Figures 5B and 5C). We also probed against the tRNA-Ala isoacceptor, which is another m2,2G-containing tRNA, but did not detect a significant change in levels between any of the cell lines (Figures 5B and 5C). We also probed against tRNA-Lys-UUU, which does not contain m2,2G, and observed no major change in abundance (Figures 5B and 5C).

We next investigated whether the presence of TRMT1 protein alone and/or the m2,2G modification is required for tRNA stability. We performed rescue experiments using re-expression of WT TRMT1 or a TRMT1 variant containing an D233A mutation in the SAM binding domain of the methyltransferase domain that is expected to reduce catalytic activity (Figure 5D). We also created a construct expressing a TRMT1 variant lacking the N-terminal mitochondrial targeting signal without or with the D233A mutation (Figure 5D, ΔM, ΔM-D233A). We generated stable cell lines in the TRMT1-KO background and confirmed re-expression of TRMT1 by immunoblotting (Figure 5E).

To validate the functional re-expression of TRMT1, we monitored the rescue of m2,2G formation in tRNA-Met-CAU and mt-tRNA-Ile-GAU. As expected, TRMT1-KO cells with

vector alone exhibited no m2,2G stop at position 26 in tRNA-Met-CAU or mt-Ile-GAU when compared to WT control cells (Figure 5F, compare lanes 1 and 2). Re-expression of WT TRMT1 in TRMT1-KO cells was able to rescue m2,2G formation in tRNA-Met-CAU or mt-Ile-GAU, as evidenced by the re-introduction of the RT block at position 26 and the reduction of readthrough products (Figure 5F, lane 3). The re-expression of TRMT1-ΔM was able to restore m2,2G modification in tRNA-Met-CAU but not mt-tRNA-Ile-GAU (Figure 5F, lane 4). Expression of TRMT1-D233A or ΔM-D233A in TRMT1-KO cell lines led to only minor restoration of m2,2G formation at position 26 in either tRNA-Met-CAU or mt-tRNA-Ile-GAU (Figure 5F, lanes 5 and 6).

Due to the m2,2G modification catalyzed by TRMT1L at position 27 in tRNA-Tyr, the m2,2G status at the upstream position 26 cannot be ascertained by primer extension in TRMT1-KO cell lines. Instead, we employed the PHA assay described above to monitor m2,2G formation at position 26. Using the PHA assay, we detected an increase in PHA probe signal for tRNA-Tyr-GUA in the TRMT1-KO cell line compared to control WT cells (Figure 5G, compare lanes 1 and 2; quantified in Figure 5H). Re-expression of TRMT1 or TRMT1-ΔM in the TRMT1-KO cell lines resulted in a reduced PHA signal, indicative of m2,2G restoration compared to TRMT1-KO cells with vector (Figure 5G, compare lane 2 to lanes 3 and 4; quantified in Figure 5H). In contrast, expression of the TRMT1-D233A or TRMT1-ΔM-D233A variant led to only a partial reduction in PHA signal in tRNA-Tyr (Figure 5G, lanes 5 and 6; quantified in Figure 5H).

We next monitored the accumulation of mature tRNA-Tyr and Ser in the TRMT1-KO cell lines re-expressing TRMT1 variants. We find that TRMT1-KO cells with vector alone exhibited decreased levels of tRNA-Tyr and tRNA-Ser relative to the control WT strain (Figure 5G, tRNA-Tyr row, compare lanes 1 and 2; quantified in Figure 5H). Re-expression of WT TRMT1 or TRMT1-ΔMTS in TRMT1-KO cells was able to rescue tRNA-Tyr and tRNA-Ser levels back to WT control levels (Figure 5G, compare lane 2 to lanes 3 and 4; quantified in Figure 5H). In contrast, expression of the TRMT1-D233A mutants was unable to rescue tRNA-Tyr or tRNA-Ser levels in the TRMT1-KO cell line (Figure 5G, lanes 5 and 6; quantified in Figure 5H). Altogether, these results uncover a key role for TRMT1-catalyzed m2,2G modifications in the cellular stability of tRNA-Tyr and Ser isoacceptors.

Human cells with pathogenic TRMT1 variants exhibit perturbations in tRNA-Tyr and Ser levels

Homozygosity of pathogenic variants in *TRMT1* has been shown to cause nearly complete loss of m2,2G modifications in human patients with ID disorders.[25,31] Our findings described above indicate that a decrease in m2,2G modifications could impact the levels of tRNA-Tyr and tRNA-Ser in human patient cells within a disease setting. Thus, we monitored the levels of tRNA-Tyr and tRNA-Ser in human patient cell lines containing biallelic TRMT1 variants that are associated with ID disorders (Figure 6A).[25–31] Patients 1.1, 1.2, 14, 8, 19, 0, and 16 in this panel have inherited TRMT1 variants that cause aberrant splicing, reduced TRMT1 expression, and/or loss of TRMT1 activity (Figure 6A, noted in red). Patient 4 is heterozygous for a non-pathogenic TRMT1 missense allele that does not impact m2,2G levels, while Patient 14f is the heterozygous father of patient 14 who

contains a WT allele of TRMT1 and does not exhibit a major change in m2,2G modification levels. The patient cell lines were compared to control cell lines from four healthy, unrelated individuals containing WT alleles of TRMT1 (Figure 6A, C1–C4).

We first validated that m2,2G levels were decreased in the patient cell lines using the PHA assay against tRNA-Ala. All patient cell lines except for the patient 14f and 4 cell lines exhibited an increased PHA signal for tRNA-Ala relative to the control patient samples (Figure 6B; quantified in Figure 6C). In addition, we found that all patient cell lines except for patient 4 and 14f exhibited an increase in PHA signal for tRNA-Tyr relative to control cell lines, indicative of loss of m2,2G formation in tRNA-Tyr (Figure 6B; quantified in Figure 6D). Notably, we found that tRNA-Tyr and tRNA-Ser levels are reduced in all patient cell lines exhibiting deficits in m2,2G modification caused by pathogenic TRMT1 variants (Figure 6B; quantified in Figures 6E and 6F). Consistent with our finding that TRMT1 does not affect tRNA-Ala levels, no significant changes in tRNA-Ala were detected between any of the patient versus control cell lines (Figures 6B and 6G). These findings show that loss of m2,2G modification across a spectrum of individuals with pathogenic TRMT1 variants impacts serine and tyrosine tRNA levels in a physiological context of human neurodevelopmental disorders.

TRMT1 and TRMT1L are required for efficient translation of tyrosine and serine codons

The preceding results suggest that TRMT1- and/or TRMT1L-catalyzed tRNA modifications could affect the translation of tyrosine and serine codons by ensuring proper levels of functional tRNA-Tyr and tRNA-Ser. Thus, we investigated the possible effects of TRMT1 and TRMT1L on protein synthesis using codon-dependent reporter constructs. We generated mammalian expression reporters encoding nanoluciferase protein fused downstream of 10 consecutive tyrosine or serine codons (Figure 7A). The reporter constructs also contain a cassette encoding firefly luciferase expressed from a separate promoter to control for transfection efficiency (Figure 7A).

Based upon this system, we found that TRMT1-KO cells exhibited a decrease in expression of the tyrosine UAC and UAU codon reporter relative to control WT cells, with the UAC reporter exhibiting a significant reduction (Figure 7B, TRMT1-KO). We also observed a decrease in translation of the UAC tyrosine codon reporter in the TRMT1L-KO cell line, but this difference did not reach statistical significance (Figure 7B, TRMT1L-KO). The TRMT1-TRMT1L DKO cell line exhibited an even further reduction in translation of the tyrosine UAC and UAU codon reporters, indicative of an additive decrease when both TRMT1 and TRMT1L are absent (Figure 7B, DKO).

Similar to the tyrosine codon reporters, the TRMT1-KO cell line exhibited a reduction in translation for each of the serine codon reporters that was most pronounced with the serine AGU codon reporter (Figure 7C, TRMT1-KO). We note that the AGU codon is decoded by the tRNA-Ser-GCU isoacceptor family, which exhibits decreased levels in the TRMT1-KO cell line. The TRMT1L-KO cell line displayed a similar level of expression for each of the serine codon reporters as the control WT cell line (Figure 7C, TRMT1L-KO). The lack of change is consistent with a role for TRMT1L in the modification of tRNA-Tyr but not tRNA-Ser isoacceptors. Except for the serine UCC reporter, the DKO cell lines exhibited

a similar decrease in translation for the serine codon reporters as the TRMT1-KO cell line (Figure 7C, DKO). Altogether, these results suggest that the decrease in tRNA-Tyr and tRNA-Ser levels in TRMT1-KO cells reduces the translation efficiency of cognate codons, while TRMT1L-catalyzed modification has an additive effect with TRMT1 on the activity of tRNA-Tyr isoacceptors.

DISCUSSION

While the presence of m2,2G at positions 26 and 27 in mammalian tyrosine tRNAs has been known for decades, the enzyme responsible for modifying guanosine at position 27 has been elusive.[23,46,47] Here, we demonstrate that TRMT1L catalyzes m2,2G formation at position 27 in human tyrosine tRNAs. Concurrent with the work described here, Hwang et al. also report that human TRMT1L is required for m2,2G modification in tyrosine tRNAs and plays an unexpected role in acp3U modification.[59] Together, our parallel studies share and corroborate each other's main findings on TRMT1L.

TRMT1L orthologs have been identified in all sequenced vertebrates but not in invertebrates, plants, or single-cell organisms.[25,32] TRMT1L could have arisen from a gene duplication event in vertebrates from an ancestral Trm1 homolog and evolved to modify position 27 in tyrosine tRNAs. Interestingly, TRMT1L-deficient mice exhibit altered motor coordination and aberrant behavior without any major anatomical changes.[60] Moreover, TRMT1L represents one of several genes that has undergone shifts in expression within the cerebellum of certain mammals.[61] TRMT1 and TRMT1L also exhibit changes in their subcellular localization in human neural cells upon neuronal activation.[25] These findings suggest that the advent of TRMT1L and changes in its expression pattern could underlie alterations in motor control function among vertebrates. Our identification of a pathogenic TRMT1L variant associated with motor neuropathy and leukodystrophy in human patients provides key support for this conclusion and uncovers a role for acp3U modification in the nervous system.

While more than half of all tRNA isodecoders are modified by TRMT1, our studies reveal tyrosine and serine tRNAs as being exquisitely dependent upon TRMT1-catalyzed m2,2G modification for stability and accumulation. This result mirrors findings in yeast showing that destabilization of the acceptor and T stems of tRNA-Ser or tRNA-Tyr cause recognition and degradation by the rapid tRNA decay pathway.[62,63] The presence of m2,2G modification in tRNA-Tyr and tRNA-Ser could be important for preventing alternative folding patterns, as proposed previously.[15] In the absence of TRMT1-catalyzed tRNA modifications, tyrosine and serine tRNAs might fold into alternative conformations with destabilized stems, leading to the recognition and degradation of the hypomodified tRNAs. It will be interesting to determine the pathways that recognize hypomodified serine and tyrosine tRNAs in human cells, since much less is known about tRNA surveillance pathways outside of yeast and bacteria.

Notably, the levels of acp3U modification in certain tRNAs appears to be sensitive to changes in TRMT1 or TRMT1L. In the case of TRMT1, the m2,2G modification catalyzed by TRMT1 could influence the folding and orientation of the D loop that affects the addition

of acp3U at position 20 by the DTWD1/2 enzymes.[55] We note prior studies in *E. coli*, which found that TrmB-catalyzed methylation of G46 to m7G promotes acp3U formation at position U47.[56] TRMT1L could also facilitate acp3U formation in tRNA-Ala and tRNA-Cys through interaction with the tRNA substrates of DTWD1 and/or modulation of DTWD1 activity, since neither tRNA-Ala nor tRNA-Cys contain G at position 27 for modification by TRMT1L. Our studies suggest that TRMT1L exerts separable activities required for m2,2G and acp3U modification in distinct tRNA substrates. Alternatively, TRMT1L could play an indirect role in acp3U formation through changes in gene expression that reduce DTWD1 protein levels or factors that regulate DTWD1 activity.

Our findings using reporter assays indicate that TRMT1 and TRMT1L-catalyzed modifications in tRNA can influence the translation of certain tyrosine and serine codons. Interestingly, depletion of tyrosine tRNAs results in impaired translation of growth and metabolic genes enriched in cognate tyrosine codons, leading to repressed proliferation.[64] The repressed proliferation associated with tRNA-Tyr depletion is consistent with the growth defect that we detected in TRMT1 KO human cell lines as well as the developmental delays observed in human patients with TRMT1 or TRMT1L deficiency.[24,26–29] By pinpointing specific tRNAs and their mechanism of dysregulation, the results presented here could guide tRNA-based strategies for rescuing phenotypes associated with neurodevelopmental disorders linked to tRNA modification deficiency.[65,66]

Limitations of the study

The OTTR-seq method can only detect a subset of modifications that cause miscoding. Thus, there could be additional modifications impacted by TRMT1 and/or TRMT1L that are missed in this study. While we confirmed that tRNA-Tyr and -Ser levels are decreased in TRMT1-ID patient cells, the impact of TRMT1 and TRMT1L on tRNAs in other tissues and developmental stages is unknown. Finally, the study does not address the potential effects of TRMT1 and TRMT1L modifications on the translation of codons besides tyrosine and serine codons.

RESOURCE AVAILABILITY

Lead contact

Requests for further information and resources should be directed to and will be fulfilled by the lead contact, Dragony Fu (dragonyfu@rochester.edu).

Materials availability

All cell lines, plasmids, and reagents generated in this study are available from the lead contact with a completed materials transfer agreement.

Data and code availability

- All RNA-seq data in this paper have been deposited in the NCBI GEO database and are publicly available as of the date of publication. The accession number is noted in the key resources table.

- Custom computer codes for tRNA sequencing analysis have been deposited on Zenodo and are publicly available as of the date of publication. The accession number is noted in the key resources table.
- Any additional information required to reanalyze the data reported in this paper is available from the lead contact upon request.

STAR★METHODS

EXPERIMENTAL MODEL AND STUDY PARTICIPANT DETAILS

293T human embryonic cell lines—293T human embryonic cells are an immortalized epithelial cell line derived from a female fetus and were obtained from ATCC (CRL-3216). The parental 293T cell lines and derivative strains were cultured in Dulbecco's Minimal Essential Medium (DMEM) supplemented with 10% fetal bovine serum (FBS), 1X penicillin and streptomycin (ThermoFisher), and 1X Glutamax (Gibco) at 37 °C with 5% CO_2 and ambient 20% O_2. Cells were passaged every 3 days with 0.25% Trypsin. The cell lines were authenticated by STR DNA profiling and confirmed negative for mycoplasma contamination by Labcorp.

Human patient cell lines—Parents and legal guardians of primary cell donors gave their consent for the publication of clinical and genetic information according to the Declaration of Helsinki, and the study was approved by The Research Ethics Committee Institute of Neurology University College London (IoN UCL) (07/Q0512/26). Institutional permission and oversight for tissue cell culture was approved by the University of Rochester Institutional Biosafety Committee.

Human control and TRMT1 variant lymphoblastoid cell lines were generated by EBV immortalization of primary human lymphocytes obtained from patient blood samples. Human lymphoblastoid cell lines (LCL) were cultured in Roswell Park Memorial Institute (RPMI) 1640 Medium containing 15% fetal bovine serum, 2 mM L-alanyl-L-glutamine (GlutaMax, Gibco) and 1% Penicillin/Streptomycin at 37 °C with 5% CO2 and 5% O2. LCLs were passaged every 3 days by dilution.

Human control, TRMT1 and TRMT1L variant fibroblast cell lines were obtained from patients by skin biopsy. Fibroblast cell lines were cultured in Dulbecco's Minimal Essential Medium (DMEM) supplemented with 10% fetal bovine serum (FBS), 1X penicillin and streptomycin (ThermoFisher), and 1X Glutamax (Gibco) at 37 °C with 5% CO_2 and 5% O_2. Cells were passaged every 3 days with 0.25% Trypsin. Neither the human LCL or fibroblast cell lines were authenticated by STR DNA profiling or tested for mycoplasma contamination.

METHOD DETAILS

Generation of CRISPR-edited cell lines—CRISPR editing was performed using plasmid pX333 (Andrea Ventura, Addgene plasmid # 64073).[73] The oligonucleotide DNA sequences encoding single guide RNA (sgRNA) targeting TRMT1 and TRMT1L were cloned into px333 using BsmB1 and BbsI (Table S3). Plasmids were transfected into human

293T embryonic cells using calcium phosphate transfection. Individual clones were by single-cell depositing into 96-well plates. The presence of CRISPR-induced deletion in either TRMT1 or TRMT1L was detected by PCR amplification and confirmed by Sanger sequencing of PCR products amplified from genomic DNA using primers TRMT1 gPCR F2 and TRMT1 gPCR R6 (Table S3). For TRMT1, we made a targeted deletion that removes nearly all of exon 2 containing the start ATG codon in the *TRMT1* gene (Data S1). For *TRMT1L*, the targeted deletion causes an in-frame deletion in exon 1 containing the start ATG codon (Data S1).

Immunoblot assays—Cell extracts and protein samples were loaded onto BOLT 4–12% Bis-Tris gels (ThermoFisher) followed by immunoblotting onto Immobilon-FL PVDF membrane (Millipore Sigma IPFL00010). Membranes were blocked with Odyssey blocking buffer for 1 h at room temperature followed by probing with primary and secondary antibodies. Immunoblots were scanned using direct infrared fluorescence via the Odyssey system (LI-COR Biosciences). Image analysis of immunoblots were performed using Image Studio software (Li-Cor).

OTTR-seq library preparation—RNA 3′ de-phosphorylation was carried out as previously described[74] using 500 ng of total RNA from each sample. Briefly, samples were treated with T4 Polynucleotide Kinase (T4 PNK; New England Biolabs) in a modified 5x reaction buffer (350 mM Tris-HCl, pH 6.5, 50 mM MgCl2, 5 mM dithiothreitol) under low pH conditions in the absence of ATP for 30 min. OTTR-seq libraries were generated as previously described.[33] Briefly, total PNK-treated RNA was 3′ tailed using mutant BoMoC RT in buffer containing only ddATP for 90 min at 30°C, with the addition of ddGTP for another 30 min at 30°C. This was then heat-inactivated at 65°C for 5 min, and unincorporated ddATP/ddGTP was hydrolyzed by incubation in 5 mM MgCl2 and 0.5 units of shrimp alkaline phosphatase (rSAP) at 37°C for 15 min. 5 mM EGTA was added and incubated at 65°C for 5 min to stop this reaction. Reverse transcription was then performed at 37°C for 30 min, followed by heat inactivation at 70°C for 5 min. The remaining RNA and RNA/DNA hybrids were then degraded using 1 unit of RNase A at 50°C for 10 min cDNA was then cleaned up using a MinElute Reaction CleanUp Kit (Qiagen). To reduce adaptor dimers, cDNA was run on a 9% UREA page gel, and the size range of interest was cut out and eluted into gel extraction buffer (300 mM NaCl, 10 mM Tris; pH 8.0, 1 mM EDTA, 0.25% SDS) and concentrated using EtOH precipitation. Size-selected cDNA was then PCR amplified for 12 cycles using Q5 High-fidelity polymerase (NEB #M0491S). Amplified libraries were then run on a 6% TBE gel, and the size range of interest was extracted to reduce adaptor dimers further. Gel slices were eluted into gel extraction buffer (300 mM NaCl, 10 mM Tris; pH 8.0, 1 mM EDTA) followed by concentration using EtOH precipitation. Final libraries were pooled and sequenced on an Illumina NextSeq 500 150-cycle high-output kit.

Data processing—Sequencing adaptors were trimmed from raw reads using cutadapt, v1.18, and read counts were generated for small RNA types using tRAX.[68] Briefly, trimmed reads were mapped to the mature tRNAs of GRCh38/hg38 human genome assembly obtained from GtRNAdb[34,75] and the reference genome sequence using Bowtie2 in very-

sensitive mode with the following parameters to allow for a maximum of 100 alignments per read: –very-sensitive –ignore-quals –np 5 -k 100. Mapped reads were filtered to retain only the "best mapping" alignments. Raw read counts of tRNAs and other small RNA types were computed using tRNA annotations from GtRNAdb, and annotations from GENCODE M23 and miRBase v22.[76] Raw read counts were then normalized using DESeq2. Downstream data visualizations were generated with custom Python scripts using the standard tRAX output files as input. Primary data can be accessed on the GEO database.

Modification-induced misincorporations—To determine sites of potential tRNA modifications present in the sequencing data, a custom Python script was used with the tRAX output files as the input (https://github.com/Aimann/tMAP). Briefly, tRNA transcripts were filtered to have at least 20 reads encompassing the length of the tRNA transcript and must contain ≥80% uniquely mapped reads to an individual tRNA. Per-base read coverage was calculated for each of these transcripts and the counts of adenines, guanines, cytosines, thymines, and deletions were summed, and the number of non-reference bases was calculated. The number of non-reference bases was then divided by the total read coverage at that position to determine the misincorporation rate at that position. Downstream data visualizations were generated with a custom python script using these mismatch values for each tRNA, across each tissue.

We used differences in the misincorporation signature to distinguish between m2G versus m2,2G at position 26 in tRNAs. In particular, m2,2G causes a generally higher misincorporation rate compared to m2G. Moreover, we have found that m2G causes a larger ratio of T to C incorporation than m2,2G where the ratio of T to C is more even. In addition, the m2,2G modification occasionally leads to an A or deletion.

RNA analysis—RNA was extracted using TRIzol LS reagent (Invitrogen). RNAs were diluted into formamide load buffer, heated to 95°C for 3 min, and fractionated on a 10% polyacrylamide, Tris-Borate-EDTA (TBE) gel containing 7 M urea. Sybr Gold nucleic acid staining (Invitrogen) was conducted to identify the RNA pattern. RNA was subsequently transferred to a Hybond N+ membrane (GE Healthcare Life Sciences) for probe hybridization with radiolabeled oligonucleotides (Table S3). Blots were stripped by incubation at 75°C with stripping buffer (0.15 M NaCl, 0.015 M Na-citrate, 0.1% SDS) and repeated at least twice until there was no detectable signal. For quantification, tRNA levels were normalized using U6 snRNA as a loading control. PHA quantification represents the ratio of PHA versus control probe signal expressed relative to the control-WT cell line.

For primer extension analysis, 1.5 μg of total RNA was pre-annealed with 5'-^{32} P-labeled oligonucleotide and 5x hybridization buffer (250 mM Tris, pH 8.5, and 300 mM NaCl) in a total volume of 7 μL. The mixture was heated at 95°C for 3 min followed by slow cooling to 42°C. An equal amount of extension mix consisting of avian myeloblastosis virus reverse transcriptase (Promega), 5x AMV buffer and 40 μM dNTPs was added. The mixture was then incubated at 42°C for 1 h and loaded on 15% 7 M urea denaturing polyacrylamide gel. Gels were exposed on a phosphor screen (GE Healthcare) and scanned on a Bio-Rad personal molecular imager or Azure Sapphire Biomolecular Imager followed by analysis

using NIH ImageJ software. Primer extension oligonucleotide sequences were previously described[24] or in Table S3.

Purification of tRNAs—RNA was extracted from HEK 293T cell lines by TRIzol LS reagent. Small RNA (<200 nucleotides) was then purified using RNA Clean and Concentrator Zymo-Spin IC Columns (Zymo Research). RNA and 5′ biotin-oligos (Table S3) were boiled in of 95 °C for 3 min in hybridization buffer (60mM NaCl, 50mM Tris pH8.5), followed by slow cooling to 25 °C (room temperature). Dynabeads MyOne Streptavidin C1 (Invitrogen, 65001) was washed in 6X SSC (0.9M Sodium chloride, 90 mM sodium citrate), then applied to the RNA-oligo mixture for 3 h at 25 °C (room temperature). Beads were separated from the flowthrough using a magnetic rack, and the beads were washed 3 times in 3xSSC followed by 2 times in 1xSSC. Then RNase-free water was added to elute the purified RNA from the resin at 65 °C. The elution step was repeated 3 times and combined for LC-MS analysis.

Liquid chromatography-mass spectrometry—RNAs were digested and processed by LC-MS as described previously.[77] Briefly, ribonucleosides were separated using a Hypersil GOLDTM C18 Selectivity Column (Thermo Scientific) followed by nucleoside analysis using a Q Exactive Plus Hybrid Quadrupole-Orbitrap. The modification ratio was calculated using the m/z intensity values of each modified nucleoside following normalization to the sum of intensity values for the canonical nucleosides; A, U, G and C.

For molar quantification of RNA modifications by SILIS, we enzymatically digested isolated isoacceptors to their nucleoside form using a mixture of Sigma Aldrich Bioultra Alkaline Phosphatase from bovine intestinal mucosa, Sigma Aldrich Benzonase Nuclease and Merck Phosphodiesterase I. Digestion was performed for 2h at 37°C and digests were filtered through a 10 kDa MWCO plate filter at 4°C and 3000 rcf for 15 min. Samples were coinjected with 1 μL of stable isotope labeled internal standard (SILIS) derived from metabolically labeled yeast tRNA as described previously.[50] Modified nucleosides were identified and quantified using mass spectrometry. An Agilent 1290 Infinity II equipped with a diode-array detector (DAD) combined with an Agilent Technologies G6470A Triple Quad system and electrospray ionization (ESI-MS, Agilent Jetstream) was used.

Nucleosides were separated using a Synergi Fusion-RP column (Synergi 2.5 μm Fusion-RP 100 Å, 150 × 2.0 mm, Phenomenex, Torrance, CA, USA). LC buffer consists of 5 mM NH4OAc pH 5.3 (buffer A), and pure acetonitrile (buffer B) were used as buffers. The gradient starts with 100% buffer A for 1 min, followed by an increase to 10% buffer B over a period of 4 min. Buffer B is then increased to 40% over 2 min and maintained for 1 min before switching back to 100% buffer A over a period of 0.5 min and re-equilibrating the column for 2.5 min. The total time is 11 min, and the flow rate is 0.35 mL/min at a column temperature of 35°C.

An ESI source was used for ionization of the nucleosides (ESI-MS, Agilent Jetstream). The gas temperature (N2) was 230°C with a flow rate of 6 L/min. Sheath gas temperature was 400°C with a flow rate of 12 L/min. Capillary voltage was 2500 V, skimmer voltage was 15

V, nozzle voltage was 0 V, and nebulizer pressure was 40 Psi. The cell accelerator voltage was 5 V. For quantification, a DMRM and positive ion mode was used (Table S4).

Plasmids—The pcDNA3.1-TRMT1-FLAG construct was previously described.[24] The open reading frame for TRMT1 was cloned into pcDNA3.1-Twin-Strep to yield pcDNA3.1-TRMT1-Strep. The ORF for TRMT1L (GenBank: NM_030934.5) was PCR amplified from cDNA plasmid HsCD00337317 (Plasmid Repository, Harvard Medical School) and cloned into either pcDNA3.1-TWIN-Strep or pcDNA3.1–3xFLAG. The pcDNA3.1-TRMT1-Strep-D233A and pcDNA3.1-Strep-TRMT1L-D373A expression constructs were generated by DpnI site-directed mutagenesis using oligonucleotides in Table S3.

For lentiviral expression, the open reading frame for TRMT1 or TRMT1-D233A was cloned into pLenti CMV GFP Blast (659–1).[78] For lentiviral expression of TRMT1L, the open reading frame for TRMT1L or TRMT1L-D373A was PCR amplified and cloned into pLenti CMV GFP Puro (658–5). pLenti CMV GFP Blast (659–1) (Addgene plasmid #17445) and pLenti CMV GFP Puro (658–5) (Addgene plasmid #17448) were gifts from Eric Campeau and Paul Kaufman. Cloning was performed using the T5 exonuclease-dependent assembly method.[79] All plasmid constructs have been verified by whole plasmid sequencing (Plasmidsaurus).

Generation of stable cell lines—To generate lentivirus, 2.5×10^5 293T cells were seeded onto 60 × 15 mm tissue culture dishes. Then, 1.25 μg of lentiviral transfer plasmids along with a lentiviral packaging cocktail containing 0.75 μg of psPAX2 packaging plasmid and 0.5 μg of pMD2.G envelope plasmid was transfected into the 293T cells using calcium phosphate transfection. In all, 48 h after transfection, media containing virus was collected and filtered sterilized through 0.45 μm filters and flash frozen in 1 mL aliquots.

For lentiviral infection in 293T cell lines, 2.5×10^5 cells were seeded in six-well plates. 24 hours after initial seeding, 1 mL of virus (or media for mock infection) along with 2 mL of media supplemented with 10 μg/mL of polybrene was added to each well. The cells were washed with PBS and fed fresh media 24 h post-infection. Blasticidin or puromycin selection begun 48 h after infection at a concentration of 2 μg/mL. Fresh media supplemented with blasticidin or puromycin was added every other day and continued until the mock infection had no observable living cells. Stable integration and expression of each construct was verified via immunoblotting.

Transient transfection and protein purification—293T cells were transfected via calcium phosphate transfection method. Briefly, 2.5×10^6 cells were seeded on 10 cm^2 tissue culture grade plates followed by transfection with 10 μg of plasmid DNA (empty pcDNA3.1, pcDNA3.1-TRMT1-Strep or pcDNA3.1-Strep-TRMT1L). Cells were harvested 48 h later by trypsin and neutralization with media, followed by centrifugation of the cells at 700 × g for 5 min followed by subsequent PBS wash and a second centrifugation step.

Proteins were extracted by the Hypotonic Lysis protocol immediately after cells were harvested post-transfection. Cell pellets were resuspended in 0.5 mL of a hypotonic lysis buffer (20 mM HEPES pH 7.9, 2 mM MgCl2, 0.2 mM EGTA, 10% glycerol, 0.1 mM

PMSF, 1 mM DTT) per plate. Cells were kept on ice for 5 min and then underwent three freeze-thaw cycles. NaCl was added to the extracts to a concentration of 0.4 M. After incubation on ice for 5 mins, the lysates were spun down at 14,000 × g for 15 min at 4 °C. The supernatant extract was removed, and an equal volume of Hypotonic Lysis buffer supplemented with 0.2% NP-40 was added to achieve the final whole cell lysates.

Purification of Strep-tagged proteins was carried out as previously described.[80] Briefly, cell lysates from the transiently-transfected cell lines were incubated with 50 μL of MagStrep "type3" XT beads (IBA Life Sciences) for 2 h at 4 °C. Magnetic resin was washed three times in 20 mM HEPES pH 7.9, 2 mM MgCl2, 0.2 mM EGTA, 10% glycerol, 0.1% NP-40, 0.2 M NaCl, 0.1 mM PMSF, and 1 mM DTT. Proteins were eluted with 1X Buffer BX (IBA LifeSciences) containing 10 mM D-biotin. Purified proteins fractionated on a 4–12% NuPAGE Bis-Tris polyacrylamide gel (ThermoFisher), stained with SYPRO Ruby Protein Gel Stain, and imaged on an Azure Sapphire Biomolecular Imager.

***In vitro* methyltransferase assays—**DNA templates for *in vitro* transcription were generated by PCR. A list of double-stranded gBlock DNA (IDT) used as PCR templates are listed in Table S3. Each template was designed with a T7 promoter upstream of the tRNA gene sequence. Each template was PCR amplified using a T7 Forward Primer and a specific reverse primer complementary to the 3′ end of each tRNA species. PCR amplification was done using Herculase II Fusion DNA Polymerase (Agilent Technologies). The PCR parameters are as follows: 95 °C for 2 min followed by 35 cycles of 95 °C for 20 s, 48 °C for 20 s and 72 °C for 30 s, ending with 72 °C for 2 min. The PCR products were then resolved on a 2% agarose gel where bands were excised, and DNA was purified using the Qiagen Gel Extraction Kit. *In vitro* transcription was done using Optizyme T7 RNA Polymerase (ThermoFisher) following standard procedures. Reactions were incubated at 37 °C for 3 h followed by DNase treatment (RQ1 DNase, Promega) at 37 °C for 30 min. RNA was then purified using RNA Clean and Concentrator Zymo-Spin IC Columns (Zymo Research). tRNA transcripts were visualized on a 15% polyacrylamide, 7 M urea gel stained with SYBR Gold nucleic acid stain.

Prior to incubation with purified protein from human cells, the tRNA was first refolded by initial denaturation in 5 mM Tris pH 7.5 and 0.16 mM EDTA and heated to 95 °C for 2 min before a 2-min incubation on ice. Refolding was conducted at 37 °C for 20 min in the presence of HEPES pH 7.5, MgCl2, and NaCl. For each methyltransferase reaction, 100 ng of refolded tRNA was incubated with 25 nM of purified protein elution along with 50 mM TRIS pH 7.5, 0.1 mM EDTA, 1 mM DTT, 0.5 mM S-adenosylmethionine (NEB) for 6 h at 30 °C. RNA was purified using RNA Clean and Concentrator Zymo-Spin IC Columns where the RNA was resuspended in 6 μL of RNase-free water. RNA samples were analyzed by LC-MS or primer extension as described above.

Reporter assays—The pcDNA3.1–10xArg-Nano reporter plasmid was previously described.[80] Firefly luciferase is expressed from the same plasmid to serve as an internal control for transfection efficiency. The 10xArg codons were replaced using BamH1-Kpn1 digestion and T4 ligation with double-stranded annealed oligonucleotide fragments encoding 10X tyrosine or serine codons (Table S3).

Plasmids were expressed in 293T cells by transient transfection using Lipofectamine 3000 (Invitrogen) and protein was extracted by above procedures. Immunoblotting against the FLAG tag was used to quantify nano-luciferase translation. The signal from the nanoluciferase reporter protein (Nano) is expressed relative to firefly luciferase protein following normalization to a control reporter without the serine or tyrosine codon stretch to control for any differences in translation independent of the tyrosine or serine codons.

QUANTIFICATION AND STATISTICAL ANALYSIS

Statistical analyses and reproducibility—All statistics and graphs were performed and generated using GraphPad Prism software (Dotmatics). Where applicable, error bars represent the standard deviation. Statistical tests are noted in each figure legend. ****$p \leq 0.0001$, ***$p \leq 0.001$, **$p \leq 0.01$, *$p \leq 0.05$.

ADDITIONAL RESOURCES

NCBI Gene Expression Omnibus accession number GSE263642: https://www.ncbi.nlm.nih.gov/geo/query/acc.cgi?acc=GSE263642.

Supplementary Material

Refer to Web version on PubMed Central for supplementary material.

ACKNOWLEDGMENTS

We thank Kevin Welle and the University of Rochester Mass Spectrometry Resource Laboratory for technical assistance, Chesna Apere for the lentiviral TRMT1L plasmid, and Dr. Eric Phizicky and members of the Fu Lab for feedback on this manuscript. K.Z. was supported by an Agnes M. Messersmith and George Messersmith Dissertation Fellowship by the University of Rochester. This work was funded by NIH R01 GM141038, NIH R01 GM143145, and NSF CAREER Award 1552126 (to D.F.), the Deutsche Forschungsgemeinschaft (325871075-SFB 1309and 259130777-SFB 1177 to S.M.K.), the Wellcome Trust (WT093205MA and WT104033AIA), the Medical Research Council (MR/S01165X/1, MR/S005021/1, and G0601943), The National Institute for Health Research University College London Hospitals Biomedical Research Centre, the Rosetrees Trust, Ataxia UK, the Multiple System Atrophy Trust, Brain Research United Kingdom, Sparks Great Ormond Street Hospital Charity, Muscular Dystrophy United Kingdom (MDUK), and the Muscular Dystrophy Association (MDA USA) (to H.H.). In addition, S.E. and H.H. were supported by an MRC strategic award to establish an International Centre for Genomic Medicine in Neuromuscular Diseases (ICGNMD) (MR/S005021/1).

REFERENCES

1. El Yacoubi B, Bailly M, and de Crécy-Lagard V (2012). Biosynthesis and function of posttranscriptional modifications of transfer RNAs. Annu. Rev. Genet. 46, 69–95. 10.1146/annurev-genet-110711-155641. [PubMed: 22905870]
2. Jackman JE, and Alfonzo JD (2013). Transfer RNA modifications: nature's combinatorial chemistry playground. Wiley Interdiscip. Rev. RNA 4, 35–48. 10.1002/wrna.1144. [PubMed: 23139145]
3. Suzuki T (2021). The expanding world of tRNA modifications and their disease relevance. Nat. Rev. Mol. Cell Biol. 22, 375–392. 10.1038/s41580-021-00342-0. [PubMed: 33658722]
4. Phizicky EM, and Hopper AK (2023). The life and times of a tRNA. RNA 29, 898–957. 10.1261/rna.079620.123. [PubMed: 37055150]
5. Orellana EA, Siegal E, and Gregory RI (2022). tRNA dysregulation and disease. Nat. Rev. Genet. 23, 651–664. 10.1038/s41576-022-00501-9. [PubMed: 35681060]
6. Delaunay S, Helm M, and Frye M (2024). RNA modifications in physiology and disease: towards clinical applications. Nat. Rev. Genet. 25, 104–122. 10.1038/s41576-023-00645-2. [PubMed: 37714958]

7. Zhang W, Foo M, Eren AM, and Pan T (2022). tRNA modification dynamics from individual organisms to metaepitranscriptomics of microbiomes. Mol. Cell 82, 891–906. 10.1016/j.molcel.2021.12.007. [PubMed: 35032425]

8. Dedon PC, and Begley TJ (2022). Dysfunctional tRNA reprogramming and codon-biased translation in cancer. Trends Mol. Med. 28, 964–978. 10.1016/j.molmed.2022.09.007. [PubMed: 36241532]

9. Burgess RW, and Storkebaum E (2023). tRNA Dysregulation in Neurodevelopmental and Neurodegenerative Diseases. Annu. Rev. Cell Dev. Biol. 39, 223–252. 10.1146/annurev-cellbio-021623-124009. [PubMed: 37339680]

10. Ramos J, and Fu D (2019). The emerging impact of tRNA modifications in the brain and nervous system. Biochim. Biophys. Acta. Gene Regul. Mech. 1862, 412–428. 10.1016/j.bbagrm.2018.11.007. [PubMed: 30529455]

11. Chujo T, and Tomizawa K (2021). Human transfer RNA modopathies: diseases caused by aberrations in transfer RNA modifications. FEBS J. 288, 7096–7122. 10.1111/febs.15736. [PubMed: 33513290]

12. de Crecy-Lagard V, Boccaletto P, Mangleburg CG, Sharma P, Lowe TM, Leidel SA, and Bujnicki JM (2019). Matching tRNA modifications in humans to their known and predicted enzymes. Nucleic Acids Res. 47, 2143–2159. 10.1093/nar/gkz011. [PubMed: 30698754]

13. Hopper AK, Furukawa AH, Pham HD, and Martin NC (1982). Defects in modification of cytoplasmic and mitochondrial transfer RNAs are caused by single nuclear mutations. Cell 28, 543–550. 10.1016/0092-8674(82)90209-4. [PubMed: 7074684]

14. Bavi RS, Sambhare SB, and Sonawane KD (2013). MD simulation studies to investigate iso-energetic conformational behaviour of modified nucleosides m(2)G and m(2) 2G present in tRNA. Comput. Struct. Biotechnol. J. 5, e201302015. 10.5936/csbj.201302015. [PubMed: 24688708]

15. Steinberg S, and Cedergren R (1995). A correlation between N2-dimethylguanosine presence and alternate tRNA conformers. RNA 1, 886–891. [PubMed: 8548653]

16. Pallan PS, Kreutz C, Bosio S, Micura R, and Egli M (2008). Effects of N2,N2-dimethylguanosine on RNA structure and stability: crystal structure of an RNA duplex with tandem m2 2G:A pairs. RNA 14, 2125–2135. 10.1261/rna.1078508. [PubMed: 18772248]

17. Urbonavicius J, Armengaud J, and Grosjean H (2006). Identity elements required for enzymatic formation of N2,N2-dimethylguanosine from N2-monomethylated derivative and its possible role in avoiding alternative conformations in archaeal tRNA. J. Mol. Biol. 357, 387–399. 10.1016/j.jmb.2005.12.087. [PubMed: 16434050]

18. Dewe JM, Whipple JM, Chernyakov I, Jaramillo LN, and Phizicky EM (2012). The yeast rapid tRNA decay pathway competes with elongation factor 1A for substrate tRNAs and acts on tRNAs lacking one or more of several modifications. RNA 18, 1886–1896. 10.1261/rna.033654.112. [PubMed: 22895820]

19. Copela LA, Chakshusmathi G, Sherrer RL, and Wolin SL (2006). The La protein functions redundantly with tRNA modification enzymes to ensure tRNA structural stability. RNA 12, 644–654. 10.1261/rna.2307206. [PubMed: 16581807]

20. Vakiloroayaei A, Shah NS, Oeffinger M, and Bayfield MA (2017). The RNA chaperone La promotes pre-tRNA maturation via indiscriminate binding of both native and misfolded targets. Nucleic Acids Res. 45, 11341–11355. 10.1093/nar/gkx764. [PubMed: 28977649]

21. Porat J, Vakiloroayaei A, Remnant BM, Talebi M, Cargill T, and Bayfield MA (2023). Crosstalk between the tRNA methyltransferase Trm1 and RNA chaperone La influences eukaryotic tRNA maturation. J. Biol. Chem. 299, 105326. 10.1016/j.jbc.2023.105326. [PubMed: 37805140]

22. Bujnicki JM, Leach RA, Debski J, and Rychlewski L (2002). Bioinformatic analyses of the tRNA: (guanine 26, N2,N2)-dimethyltransferase (Trm1) family. J. Mol. Microbiol. Biotechnol. 4, 405–415. [PubMed: 12125821]

23. Liu J, and Strâby KB (2000). The human tRNA(m(2)(2)G(26))dimethyltransferase: functional expression and characterization of a cloned hTRM1 gene. Nucleic Acids Res. 28, 3445–3451. 10.1093/nar/28.18.3445. [PubMed: 10982862]

24. Dewe JM, Fuller BL, Lentini JM, Kellner SM, and Fu D (2017). TRMT1-Catalyzed tRNA Modifications Are Required for Redox Homeostasis To Ensure Proper Cellular Proliferation and

Oxidative Stress Survival. Mol. Cell Biol. 37, e00214–17. 10.1128/MCB.00214-17. [PubMed: 28784718]

25. Jonkhout N, Cruciani S, Santos Vieira HG, Tran J, Liu H, Liu G, Pickford R, Kaczorowski D, Franco GR, Vauti F, et al. (2021). Subcellular relocalization and nuclear redistribution of the RNA methyltransferases TRMT1 and TRMT1L upon neuronal activation. RNA Biol. 18, 1905–1919. 10.1080/15476286.2021.1881291. [PubMed: 33499731]
26. Blaesius K, Abbasi AA, Tahir TH, Tietze A, Picker-Minh S, Ali G, Farooq S, Hu H, Latif Z, Khan MN, and Kaindl A (2018). Mutations in the tRNA methyltransferase 1 gene TRMT1 cause congenital microcephaly, isolated inferior vermian hypoplasia and cystic leukomalacia in addition to intellectual disability. Am. J. Med. Genet. 176, 2517–2521. 10.1002/ajmg.a.38631. [PubMed: 30289604]
27. Davarniya B, Hu H, Kahrizi K, Musante L, Fattahi Z, Hosseini M, Maqsoud F, Farajollahi R, Wienker TF, Ropers HH, and Najmabadi H (2015). The Role of a Novel TRMT1 Gene Mutation and Rare GRM1 Gene Defect in Intellectual Disability in Two Azeri Families. PLoS One 10, e0129631. 10.1371/journal.pone.0129631. [PubMed: 26308914]
28. Monies D, Abouelhoda M, AlSayed M, Alhassnan Z, Alotaibi M, Kayyali H, Al-Owain M, Shah A, Rahbeeni Z, Al-Muhaizea MA, et al. (2017). The landscape of genetic diseases in Saudi Arabia based on the first 1000 diagnostic panels and exomes. Hum. Genet. 136, 921–939. 10.1007/s00439-017-1821-8. [PubMed: 28600779]
29. Najmabadi H, Hu H, Garshasbi M, Zemojtel T, Abedini SS, Chen W, Hosseini M, Behjati F, Haas S, Jamali P, et al. (2011). Deep sequencing reveals 50 novel genes for recessive cognitive disorders. Nature 478, 57–63. 10.1038/nature10423. [PubMed: 21937992]
30. Efthymiou S, Leo CP, Deng C, Zhang K, Lin S-J, Maroofian R, Kaiyrzhanov R, Lin R, Karagoz I, Scardamaglia A, et al. (2024). Biallelic pathogenic variants in TRMT1 disrupt tRNA modification and induce a syndromic neurodevelopmental disorder. Preprint at medRxiv. 10.1101/2024.07.18.24310581.
31. Zhang K, Lentini JM, Prevost CT, Hashem MO, Alkuraya FS, and Fu D (2020). An intellectual disability-associated missense variant in TRMT1 impairs tRNA modification and reconstitution of enzymatic activity. Hum. Mutat. 41, 600–607. 10.1002/humu.23976. [PubMed: 31898845]
32. Towns WL, and Begley TJ (2012). Transfer RNA methytransferases and their corresponding modifications in budding yeast and humans: activities, predications, and potential roles in human health. DNA Cell Biol. 31, 434–454. 10.1089/dna.2011.1437. [PubMed: 22191691]
33. Upton HE, Ferguson L, Temoche-Diaz MM, Liu XM, Pimentel SC, Ingolia NT, Schekman R, and Collins K (2021). Low-bias ncRNA libraries using ordered two-template relay: Serial template jumping by a modified retroelement reverse transcriptase. Proc. Natl. Acad. Sci. USA 118, e2107900118. 10.1073/pnas.2107900118. [PubMed: 34649994]
34. Chan PP, Lin BY, Mak AJ, and Lowe TM (2021). tRNAscan-SE 2.0: improved detection and functional classification of transfer RNA genes. Nucleic Acids Res. 49, 9077–9096. 10.1093/nar/gkab688. [PubMed: 34417604]
35. Cozen AE, Quartley E, Holmes AD, Hrabeta-Robinson E, Phizicky EM, and Lowe TM (2015). ARM-seq: AlkB-facilitated RNA methylation sequencing reveals a complex landscape of modified tRNA fragments. Nat. Methods 12, 879–884. 10.1038/nmeth.3508. [PubMed: 26237225]
36. Clark WC, Evans ME, Dominissini D, Zheng G, and Pan T (2016). tRNA base methylation identification and quantification via high-throughput sequencing. RNA 22, 1771–1784. 10.1261/rna.056531.116. [PubMed: 27613580]
37. Dai Q, Zheng G, Schwartz MH, Clark WC, and Pan T (2017). Selective Enzymatic Demethylation of N^2, N^2 -Dimethylguanosine in RNA and Its Application in High-Throughput tRNA Sequencing. Angew. Chem., Int. Ed. Engl. 56, 5017–5020. 10.1002/anie.201700537. [PubMed: 28371071]
38. Zheng G, Qin Y, Clark WC, Dai Q, Yi C, He C, Lambowitz AM, and Pan T (2015). Efficient and quantitative high-throughput tRNA sequencing. Nat. Methods 12, 835–837. 10.1038/nmeth.3478. [PubMed: 26214130]
39. Hernandez-Alias X, Katanski CD, Zhang W, Assari M, Watkins CP, Schaefer MH, Serrano L, and Pan T (2023). Single-read tRNA-seq analysis reveals coordination of tRNA modification and

aminoacylation and fragmentation. Nucleic Acids Res. 51, e17. 10.1093/nar/gkac1185. [PubMed: 36537222]

40. Behrens A, Rodschinka G, and Nedialkova DD (2021). High-resolution quantitative profiling of tRNA abundance and modification status in eukaryotes by mim-tRNAseq. Mol. Cell 81, 1802–1815.e7. 10.1016/j.molcel.2021.01.028. [PubMed: 33581077]
41. Pinkard O, McFarland S, Sweet T, and Coller J (2020). Quantitative tRNA-sequencing uncovers metazoan tissue-specific tRNA regulation. Nat. Commun. 11, 4104. 10.1038/s41467-020-17879-x. [PubMed: 32796835]
42. Cui J, Liu Q, Sendinc E, Shi Y, and Gregory RI (2021). Nucleotide resolution profiling of m3C RNA modification by HAC-seq. Nucleic Acids Res. 49, e27. 10.1093/nar/gkaa1186. [PubMed: 33313824]
43. Suzuki T, Yashiro Y, Kikuchi I, Ishigami Y, Saito H, Matsuzawa I, Okada S, Mito M, Iwasaki S, Ma D, et al. (2020). Complete chemical structures of human mitochondrial tRNAs. Nat. Commun. 11, 4269. 10.1038/s41467-020-18068-6. [PubMed: 32859890]
44. Youvan DC, and Hearst JE (1979). Reverse transcriptase pauses at N2-methylguanine during in vitro transcription of Escherichia coli 16S ribosomal RNA. Proc. Natl. Acad. Sci. USA 76, 3751–3754. 10.1073/pnas.76.8.3751. [PubMed: 91169]
45. Motorin Y, Muller S, Behm-Ansmant I, and Branlant C (2007). Identification of modified residues in RNAs by reverse transcription-based methods. Methods Enzymol. 425, 21–53. 10.1016/S0076-6879(07)25002-5. [PubMed: 17673078]
46. van Tol H, Stange N, Gross HJ, and Beier H (1987). A human and a plant intron-containing tRNATyr gene are both transcribed in a HeLa cell extract but spliced along different pathways. EMBO J. 6, 35–41. 10.1002/j.1460-2075.1987.tb04715.x. [PubMed: 3502708]
47. Johnson GD, Pirtle IL, and Pirtle RM (1985). The nucleotide sequence of tyrosine tRNAQ* psi A from bovine liver. Arch. Biochem. Biophys. 236, 448–453. 10.1016/0003-9861(85)90647-2. [PubMed: 2981510]
48. Pan T (2018). Modifications and functional genomics of human transfer RNA. Cell Res. 28, 395–404. 10.1038/s41422-018-0013-y. [PubMed: 29463900]
49. Kellner S, Ochel A, Thüring K, Spenkuch F, Neumann J, Sharma S, Entian KD, Schneider D, and Helm M (2014). Absolute and relative quantification of RNA modifications via biosynthetic isotopomers. Nucleic Acids Res. 42, e142. 10.1093/nar/gku733. [PubMed: 25129236]
50. Heiss M, Borland K, Yoluc Y, and Kellner S (2021). Quantification of Modified Nucleosides in the Context of NAIL-MS. Methods Mol. Biol. 2298, 279–306. 10.1007/978-1-0716-1374-0_18. [PubMed: 34085252]
51. Arimbasseri AG, Blewett NH, Iben JR, Lamichhane TN, Cherkasova V, Hafner M, and Maraia RJ (2015). RNA Polymerase III Output Is Functionally Linked to tRNA Dimethyl-G26 Modification. PLoS Genet. 11, e1005671. 10.1371/journal.pgen.1005671. [PubMed: 26720005]
52. Khalique A, Mattijssen S, and Maraia RJ (2022). A versatile tRNA modification-sensitive northern blot method with enhanced performance. RNA 28, 418–432. 10.1261/rna.078929.121. [PubMed: 34930808]
53. Edqvist J, Grosjean H, and Stråby KB (1992). Identity elements for N2-dimethylation of guanosine-26 in yeast tRNAs. Nucleic Acids Res. 20, 6575–6581. 10.1093/nar/20.24.6575. [PubMed: 1480477]
54. Cappannini A, Ray A, Purta E, Mukherjee S, Boccaletto P, Moafinejad SN, Lechner A, Barchet C, Klaholz BP, Stefaniak F, and Bujnicki JM (2024). MODOMICS: a database of RNA modifications and related information. 2023 update. Nucleic Acids Res. 52, D239–D244. 10.1093/nar/gkad1083. [PubMed: 38015436]
55. Takakura M, Ishiguro K, Akichika S, Miyauchi K, and Suzuki T (2019). Biogenesis and functions of aminocarboxypropyluridine in tRNA. Nat. Commun. 10, 5542. 10.1038/s41467-019-13525-3. [PubMed: 31804502]
56. Meyer B, Immer C, Kaiser S, Sharma S, Yang J, Watzinger P, Weiß L, Kotter A, Helm M, Seitz HM, et al. (2020). Identification of the 3-amino-3-carboxypropyl (acp) transferase enzyme responsible for acp3U formation at position 47 in Escherichia coli tRNAs. Nucleic Acids Res. 48, 1435–1450. 10.1093/nar/gkz1191. [PubMed: 31863583]

57. Funk HM, Zhao R, Thomas M, Spigelmyer SM, Sebree NJ, Bales RO, Burchett JB, Mamaril JB, Limbach PA, and Guy MP (2020). Identification of the enzymes responsible for m2,2G and acp3U formation on cytosolic tRNA from insects and plants. PLoS One 15, e0242737. 10.1371/journal.pone.0242737. [PubMed: 33253256]
58. Sobreira N, Schiettecatte F, Valle D, and Hamosh A (2015). Gene-Matcher: a matching tool for connecting investigators with an interest in the same gene. Hum. Mutat. 36, 928–930. 10.1002/humu.22844. [PubMed: 26220891]
59. Hwang S-P, Liao H, Barondeau K, Han X, Herbert C, McConie H, Shekar A, Pestov D, Limbach PA, Chang JT, and Denicourt C (2024). TRMT1L-catalyzed m22G27 on tyrosine tRNA is required for efficient mRNA translation and cell survival under oxidative stress. Preprint at bioRxiv. 10.1101/2024.05.02.591343.
60. Vauti F, Goller T, Beine R, Becker L, Klopstock T, Hölter SM, Wurst W, Fuchs H, Gailus-Durner V, de Angelis MH, and Arnold HH (2007). The mouse Trm1-like gene is expressed in neural tissues and plays a role in motor coordination and exploratory behaviour. Gene 389, 174–185. 10.1016/j.gene.2006.11.004. [PubMed: 17198746]
61. Brawand D, Soumillon M, Necsulea A, Julien P, Csárdi G, Harrigan P, Weier M, Liechti A, Aximu-Petri A, Kircher M, et al. (2011). The evolution of gene expression levels in mammalian organs. Nature 478, 343–348. 10.1038/nature10532. [PubMed: 22012392]
62. Whipple JM, Lane EA, Chernyakov I, D'Silva S, and Phizicky EM (2011). The yeast rapid tRNA decay pathway primarily monitors the structural integrity of the acceptor and T-stems of mature tRNA. Genes Dev. 25, 1173–1184. 10.1101/gad.2050711. [PubMed: 21632824]
63. Guy MP, Young DL, Payea MJ, Zhang X, Kon Y, Dean KM, Grayhack EJ, Mathews DH, Fields S, and Phizicky EM (2014). Identification of the determinants of tRNA function and susceptibility to rapid tRNA decay by high-throughput in vivo analysis. Genes Dev. 28, 1721–1732. 10.1101/gad.245936.114. [PubMed: 25085423]
64. Huh D, Passarelli MC, Gao J, Dusmatova SN, Goin C, Fish L, Pinzaru AM, Molina H, Ren Z, McMillan EA, et al. (2021). A stress-induced tyrosine-tRNA depletion response mediates codon-based translational repression and growth suppression. EMBO J. 40, e106696. 10.15252/embj.2020106696. [PubMed: 33346941]
65. Anastassiadis T, and Köhrer C (2023). Ushering in the era of tRNA medicines. J. Biol. Chem. 299, 105246. 10.1016/j.jbc.2023.105246. [PubMed: 37703991]
66. Hou Y, Zhang W, McGilvray PT, Sobczyk M, Wang T, Weng SHS, Huff A, Huang S, Pena N, Katanski CD, and Pan T (2024). Engineered mischarged transfer RNAs for correcting pathogenic missense mutations. Mol. Ther. 32, 352–371. 10.1016/j.ymthe.2023.12.014. [PubMed: 38104240]
67. Martin M (2011). Cutadapt removes adapter sequences from high-throughput sequencing reads. Embnet 17, 3. 10.14806/ej.17.1.200.
68. Holmes AD, Howard JM, Chan PP, and Lowe TM (2022). tRNA Analysis of eXpression (tRAX): A tool for integrating analysis of tRNAs, tRNA-derived small RNAs, and tRNA modifications. Preprint at bioRxiv. 10.1101/2022.07.02.498565.
69. Langmead B, and Salzberg SL (2012). Fast gapped-read alignment with Bowtie 2. Nat. Methods 9, 357–359. 10.1038/nmeth.1923. [PubMed: 22388286]
70. Langmead B, Wilks C, Antonescu V, and Charles R (2019). Scaling read aligners to hundreds of threads on general-purpose processors. Bioinformatics 35, 421–432. 10.1093/bioinformatics/bty648. [PubMed: 30020410]
71. Love MI, Huber W, and Anders S (2014). Moderated estimation of fold change and dispersion for RNA-seq data with DESeq2. Genome Biol. 15, 550. 10.1186/s13059-014-0550-8. [PubMed: 25516281]
72. Schindelin J, Arganda-Carreras I, Frise E, Kaynig V, Longair M, Pietzsch T, Preibisch S, Rueden C, Saalfeld S, Schmid B, et al. (2012). Fiji: an open-source platform for biological-image analysis. Nat. Methods 9, 676–682. 10.1038/nmeth.2019. [PubMed: 22743772]
73. Maddalo D, Manchado E, Concepcion CP, Bonetti C, Vidigal JA, Han YC, Ogrodowski P, Crippa A, Rekhtman N, de Stanchina E, et al. (2014). In vivo engineering of oncogenic chromosomal rearrangements with the CRISPR/Cas9 system. Nature 516, 423–427. 10.1038/nature13902. [PubMed: 25337876]

74. Huppertz I, Attig J, D'Ambrogio A, Easton LE, Sibley CR, Sugimoto Y, Tajnik M, König J, and Ule J (2014). iCLIP: protein-RNA interactions at nucleotide resolution. Methods 65, 274–287. 10.1016/j.ymeth.2013.10.011. [PubMed: 24184352]

75. Chan PP, and Lowe TM (2016). GtRNAdb 2.0: an expanded database of transfer RNA genes identified in complete and draft genomes. Nucleic Acids Res. 44, D184–D189. 10.1093/nar/gkv1309. [PubMed: 26673694]

76. Kozomara A, and Griffiths-Jones S (2014). miRBase: annotating high confidence microRNAs using deep sequencing data. Nucleic Acids Res. 42, D68–D73. 10.1093/nar/gkt1181. [PubMed: 24275495]

77. Su D, Chan CTY, Gu C, Lim KS, Chionh YH, McBee ME, Russell BS, Babu IR, Begley TJ, and Dedon PC (2014). Quantitative analysis of ribonucleoside modifications in tRNA by HPLC-coupled mass spectrometry. Nat. Protoc. 9, 828–841. 10.1038/nprot.2014.047. [PubMed: 24625781]

78. Campeau E, Ruhl VE, Rodier F, Smith CL, Rahmberg BL, Fuss JO, Campisi J, Yaswen P, Cooper PK, and Kaufman PD (2009). A versatile viral system for expression and depletion of proteins in mammalian cells. PLoS One 4, e6529. 10.1371/journal.pone.0006529. [PubMed: 19657394]

79. Xia Y, Li K, Li J, Wang T, Gu L, and Xun L (2019). T5 exonuclease-dependent assembly offers a low-cost method for efficient cloning and site-directed mutagenesis. Nucleic Acids Res. 47, e15. 10.1093/nar/gky1169. [PubMed: 30462336]

80. Lentini JM, Alsaif HS, Faqeih E, Alkuraya FS, and Fu D (2020). DALRD3 encodes a protein mutated in epileptic encephalopathy that targets arginine tRNAs for 3-methylcytosine modification. Nat. Commun. 11, 2510. 10.1038/s41467-020-16321-6. [PubMed: 32427860]

Highlights

- Human TRMT1 catalyzes m2,2G modification in more than half of all tRNAs
- Human TRMT1L catalyzes m2,2G in tyrosine tRNAs while modulating acp3U in tRNAs
- Tyrosine and serine tRNAs require m2,2G modifications for stability and function
- Pathogenic variants in TRMT1 or TRMT1L cause perturbations in tRNA modification

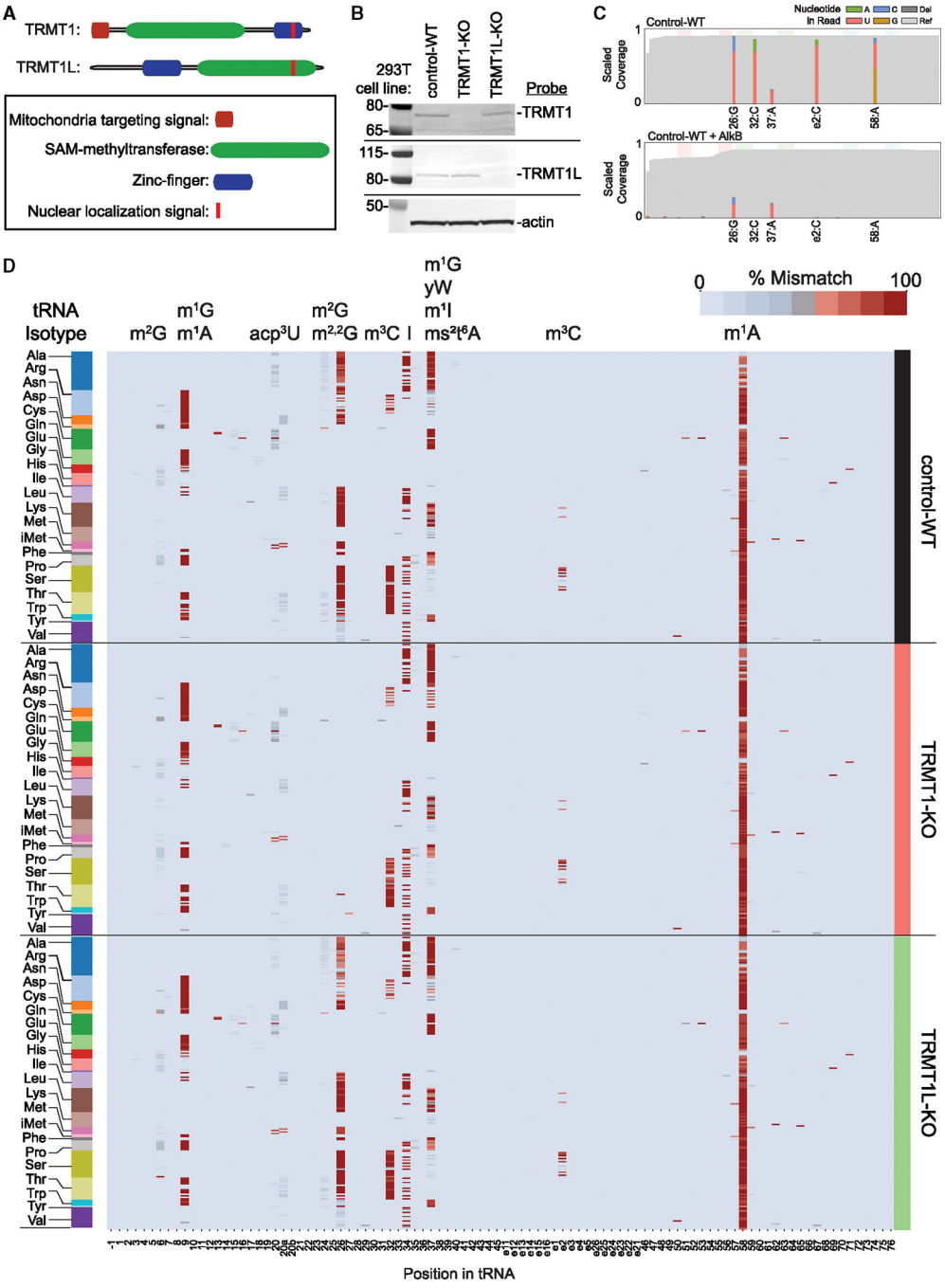

Figure 1. Mapping tRNA modifications dependent upon TRMT1 and TRMT1L

(A) TRMT1 and TRMT1L protein domains.

(B) Immunoblot of TRMT1 and TRMT1L in lysates from the indicated human cell lines.

(C) Mismatch incorporation frequency across the tRNA transcriptome in control wild-type (WT) human cells without or with (+) AlkB treatment.

(D) Heatmap of the relative mismatch incorporation frequency across the tRNA transcriptome in the human cell lines. Predicted modifications are noted above the map.

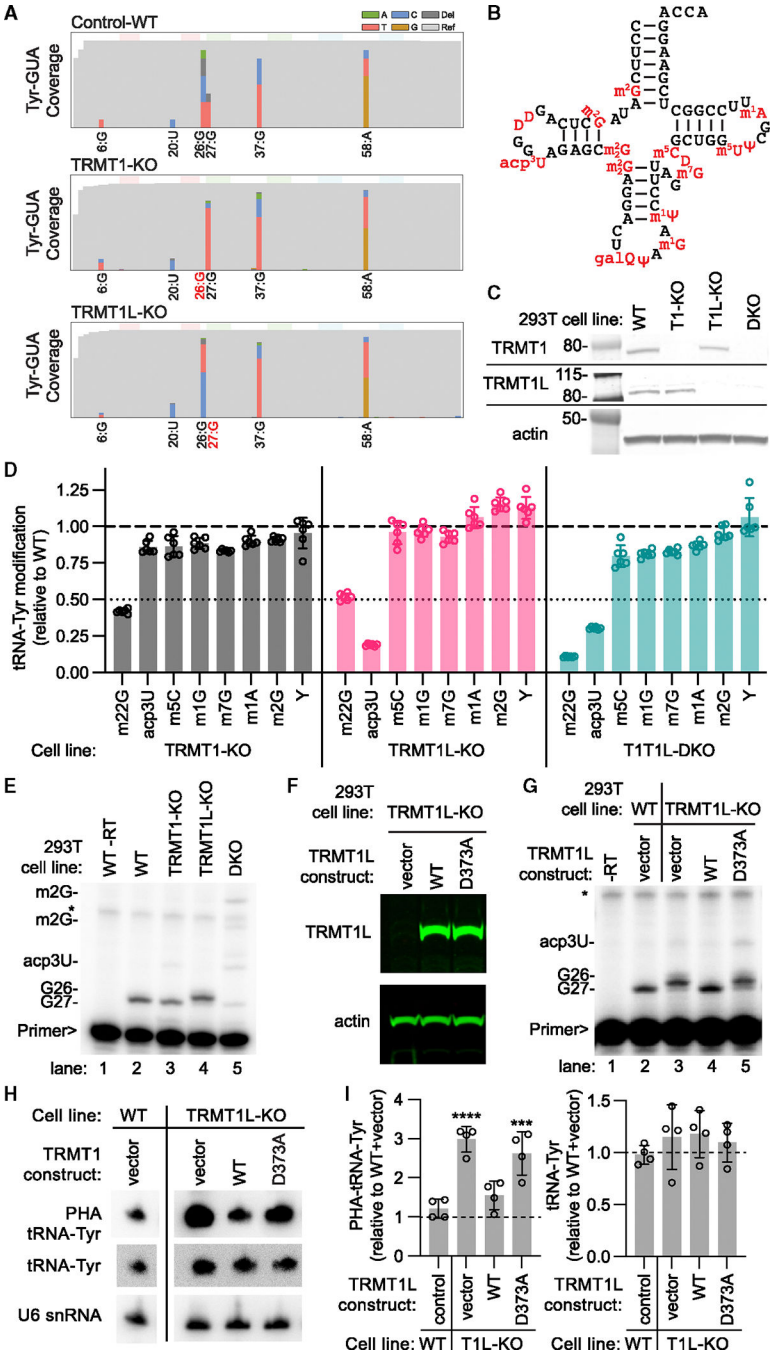

Figure 2. TRMT1 and TRMT1L catalyze m2,2G modification at positions 26 and 27 of tRNA-Tyr, respectively

(A) Misincorporation frequency for tRNA-Tyr isoacceptors from the indicated cell lines.

(B) tRNA-Tyr with known modifications.

(C) Immunoblot of TRMT1 and TRMT1L levels in the indicated cell lines.

(D) Relative peak intensity values of the indicated modifications detected by LC-MS in purified tRNA-Tyr from the cell lines versus the control WT cell line.

(E) Primer extension analysis of tRNA-Tyr from the indicated cell lines. An asterisk represents a non-specific band.

(F) Immunoblot analysis of TRMT1L expression in the TRMT1L-KO cell lines.
(G) Primer extension analysis of tRNA-Tyr from the indicated cell lines.
(H) PHA northern blot analysis to detect m2,2G at position 26.
(I) Quantification of northern blot signal in (H). Bars represent the standard deviation from the mean. Statistical analysis was performed using one-way ANOVA, and significance was calculated using Dunnett's multiple comparison test. ****$p \leq 0.0001$, ***$p \leq 0.001$.

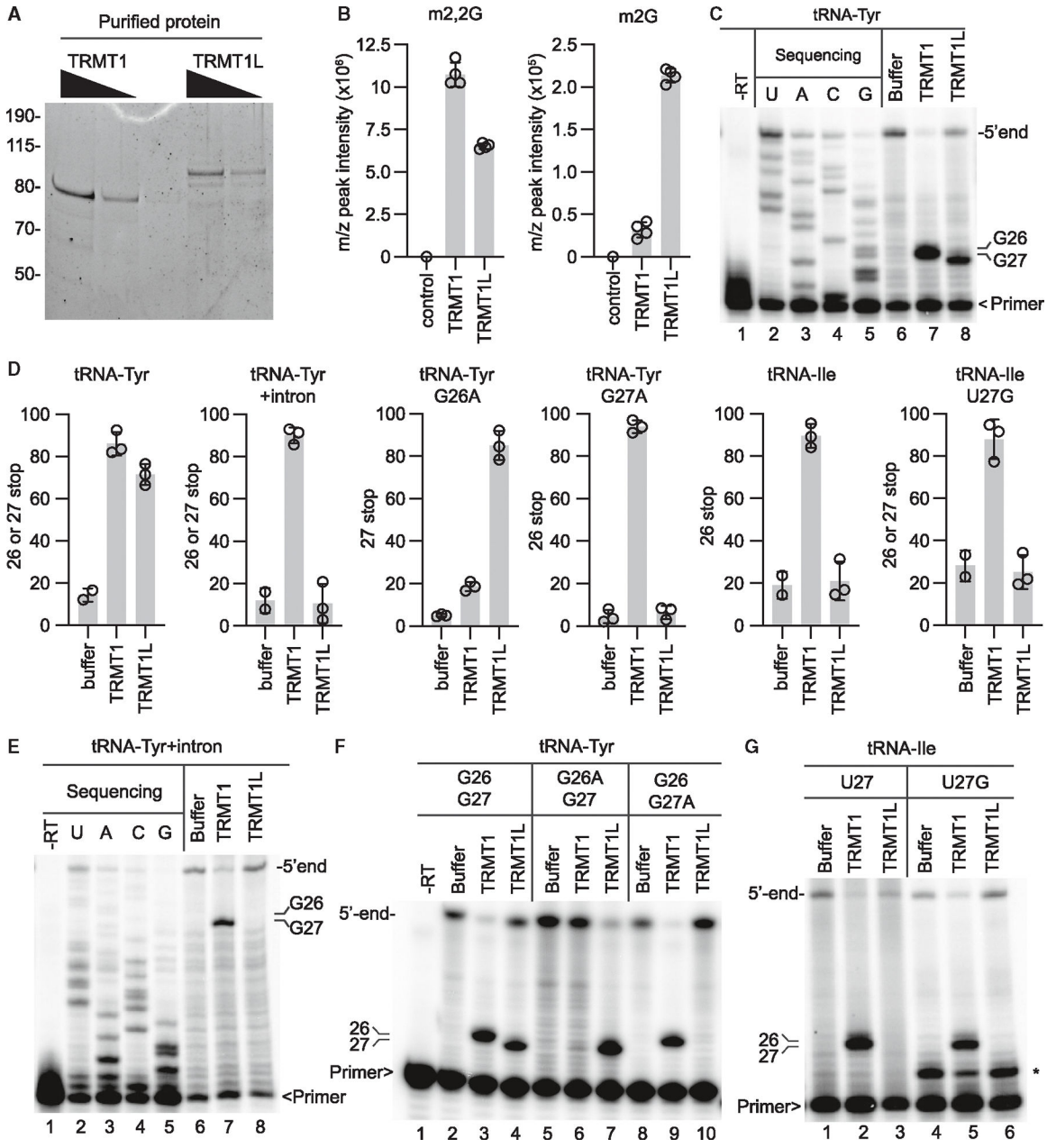

Figure 3. *In vitro* reconstitution of TRMT1 and TRMT1L methyltransferase activity on tRNA substrates

(A) Sypro Ruby-stained gel of purified TRMT1 and TRMT1L.

(B) Peak intensity areas of m2,2G or m2G measured by LC–MS in *in vitro*-transcribed tRNA-Tyr after pre-incubation with buffer control, TRMT1, or TRMT1L.

(C) Primer extension assay of tRNA-Tyr.

(D) Quantification of G26 and/or G27 stop in (C) and (E)–(G).

(E–G) Primer extension analysis of (E) intron-containing pre-tRNA-Tyr, (F) tRNA-Tyr variants, and (G) tRNA-Ile variants. An asterisk denotes a non-specific band.

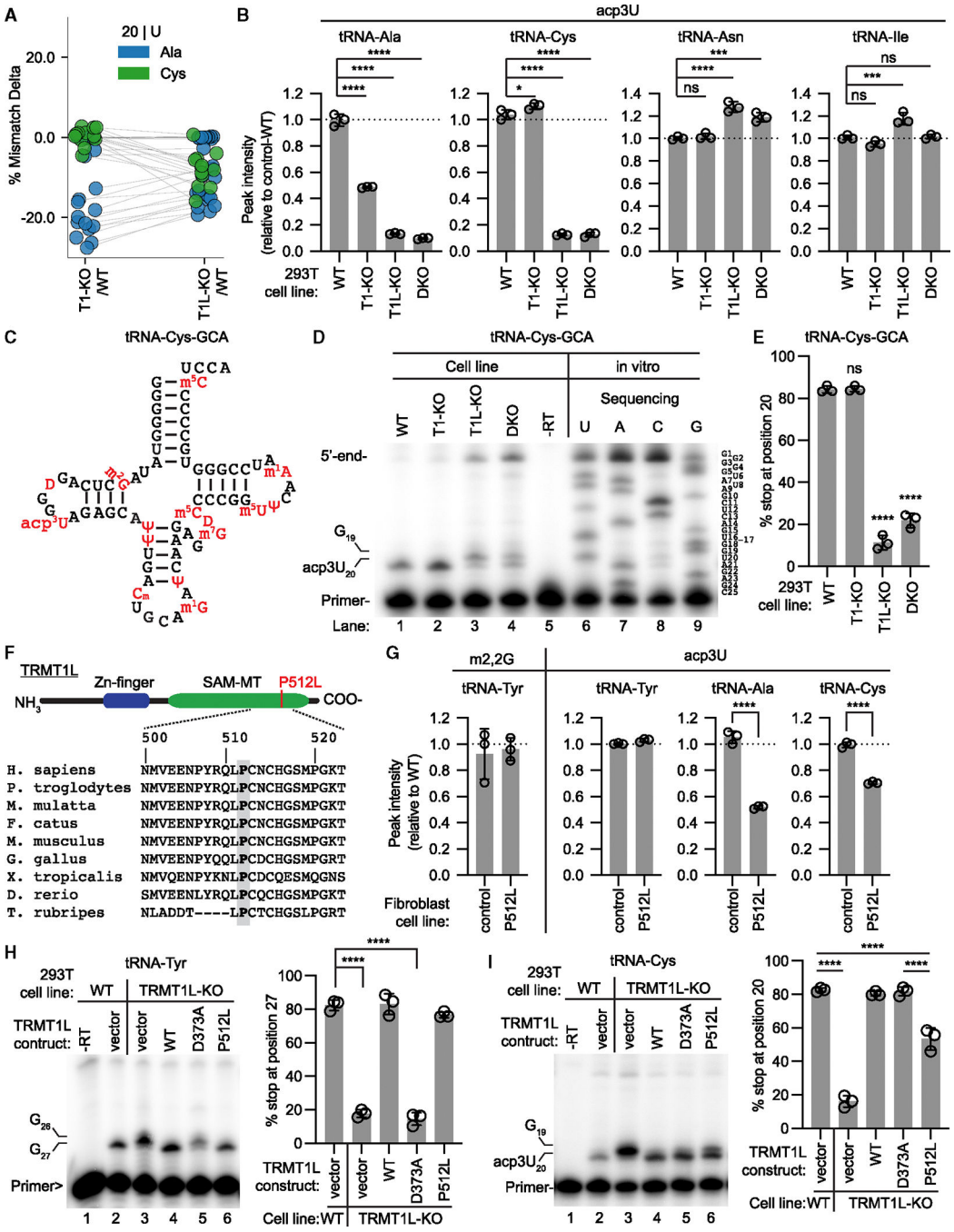

Figure 4. TRMT1- and TRMT1L-deficient human cells exhibit a reduction in acp3U modification in a subset of tRNAs

(A) Change in mismatch incorporation percentage at position U20 for tRNA-Ala or tRNA-Cys in the TRMT1-KO or TRMT1L-KO cell line relative to the control-WT cell line.

(B) Relative peak intensity values of acp3U modification detected by LC-MS in the indicated tRNAs purified from HEK293T cell lines versus control-WT.

(C) tRNA-Cys with modifications in red.

(D) Primer extension gel of tRNA-Cys from the indicated HEK293T cell lines.

(E) Quantification of the stop signal relative to readthrough plus stop signal of (D).

(F) Sequence alignment of TRMT1L homologs encompassing the P512 residue.
(G) Relative peak intensity values of the indicated modifications detected by LC-MS in purified tRNAs from fibroblast cell lines.
(H and I) Primer extension assay gels to monitor m2,2G or acp3U in tRNA-Tyr or tRNA-Cys, respectively, from the indicated cell lines with quantification of percent stop.
Statistical analysis was performed using one-way ANOVA, and significance was calculated using Dunnett's multiple comparison test for (B), (E), (G), and (H) or Tukey's multiple-comparisons test for (I). ****$p \leq 0.0001$, ***$p \leq 0.001$, **$p \leq 0.01$, *$p \leq 0.05$.

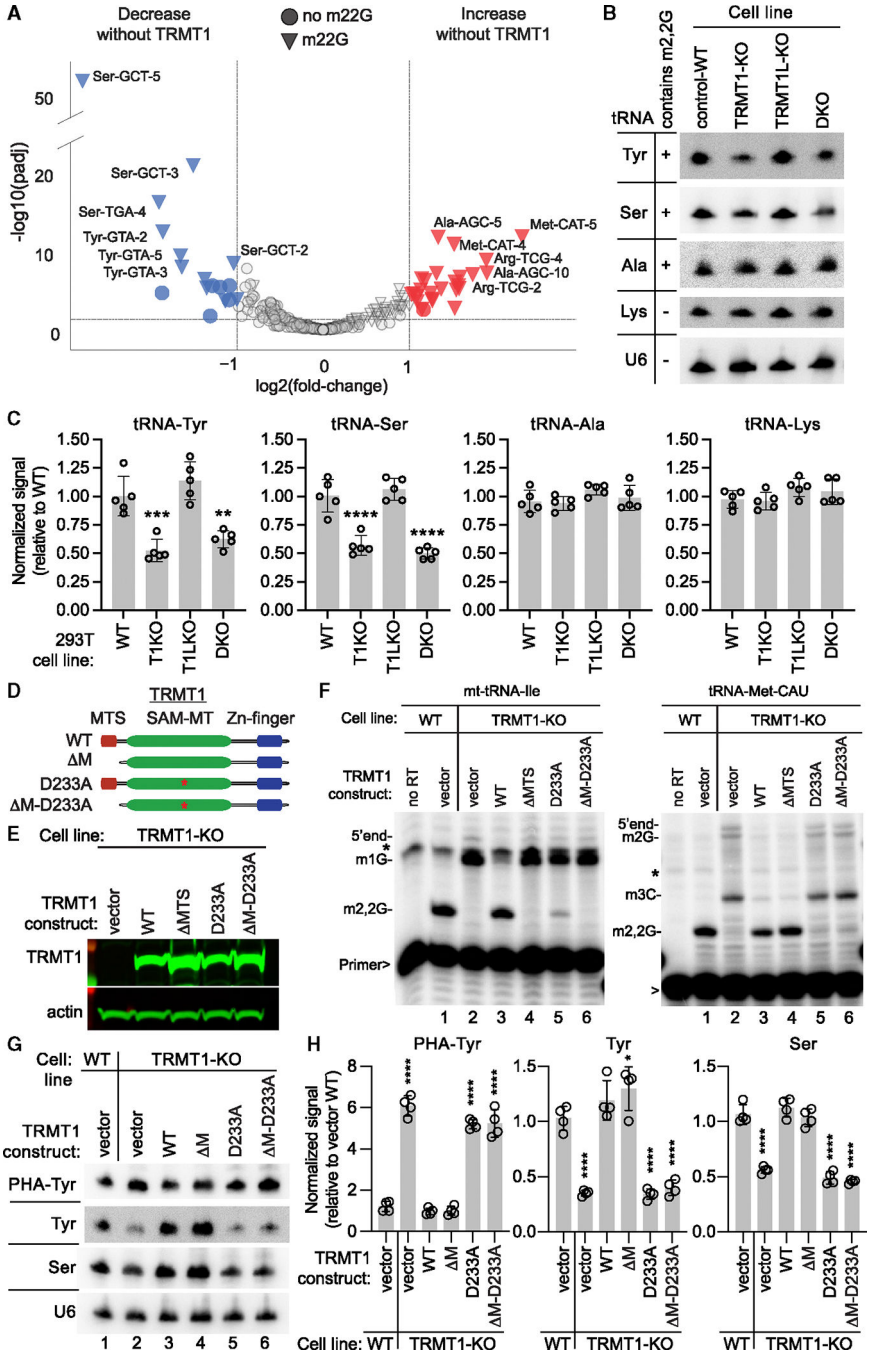

Figure 5. TRMT1-catalyzed modification is required for the accumulation of tyrosine and serine tRNAs in human cells

(A) Volcano plot of tRNA levels in TRMT1-KO versus control WT cell lines. Triangles represent tRNAs that are modified with m2,2G at position 26. Circles represent tRNAs without m2,2G. Red and blue denote tRNAs that are increased and decreased, respectively, in the TRMT1-KO cell lines.

(B) Northern blot of tRNAs from the indicated HEK293T cell lines.

(C) Quantification of northern blots in (B).

(D) Schematic of TRMT1 variants.

(E) Immunoblot analysis of TRMT1 variants in the TRMT1-KO cell line.
(F) Primer extension analysis of mt-tRNA-Ile or tRNA-Met-CAU from cell lines containing stable integration of the indicated TRMT1 construct.
(G) Northern blot of tRNAs from control WT and TRMT1-KO cell lines containing the indicated TRMT1 construct.
(H) Quantification of northern blots in (G). Bars represent the standard deviation from the mean. Statistical analysis was performed using one-way ANOVA, and significance was calculated using Dunnett's multiple-comparisons test. $****p \leq 0.0001$, $***p \leq 0.001$, $**p \leq 0.01$.

A

Patient	Allele 1	Allele 2	Genetic effect	Protein change	m2,2G in tRNA-Met
1.1	C454-1G>C	C454-1G>C	Frameshift	Cys86Gln *fs*24	Decrease
1.2	C454-1G>C	C454-1G>C	Frameshift	Cys86Gln *fs*24	Decrease
14f	Wildtype	c.691G>A	Missense	Asp231Asn	No change
14	c.691G>A	c.691G>A	Missense	Asp231Asn	Decrease
C1	Wildtype	Wildtype	Wildtype	Wildtype	No change
4	c.995A>G	c.255-1G>T	Missense, frameshift	Q332R, Cys86Gln *fs*24	No change
8	C1107-1G>A	C389_390delAA	Frameshift	Ala370Pro *fs*11, Lys130Arg *fs*3	Decrease
19	c.1400C>T	c.967C>T	Missense, frameshift	Ser467Leu, Arg323Cys	Decrease
C2	Wildtype	Wildtype	Wildtype	Wildtype	No change
0	c.967C>T	c.967C>T	Missense	Arg323Cys	Decrease
C3	Wildtype	Wildtype	Wildtype	Wildtype	No change
16	c.311-1G>A	c.311-1G>A	Frameshift	Cys86Gln *fs*24	Decrease
C4	Wildtype	Wildtype	Wildtype	Wildtype	No change

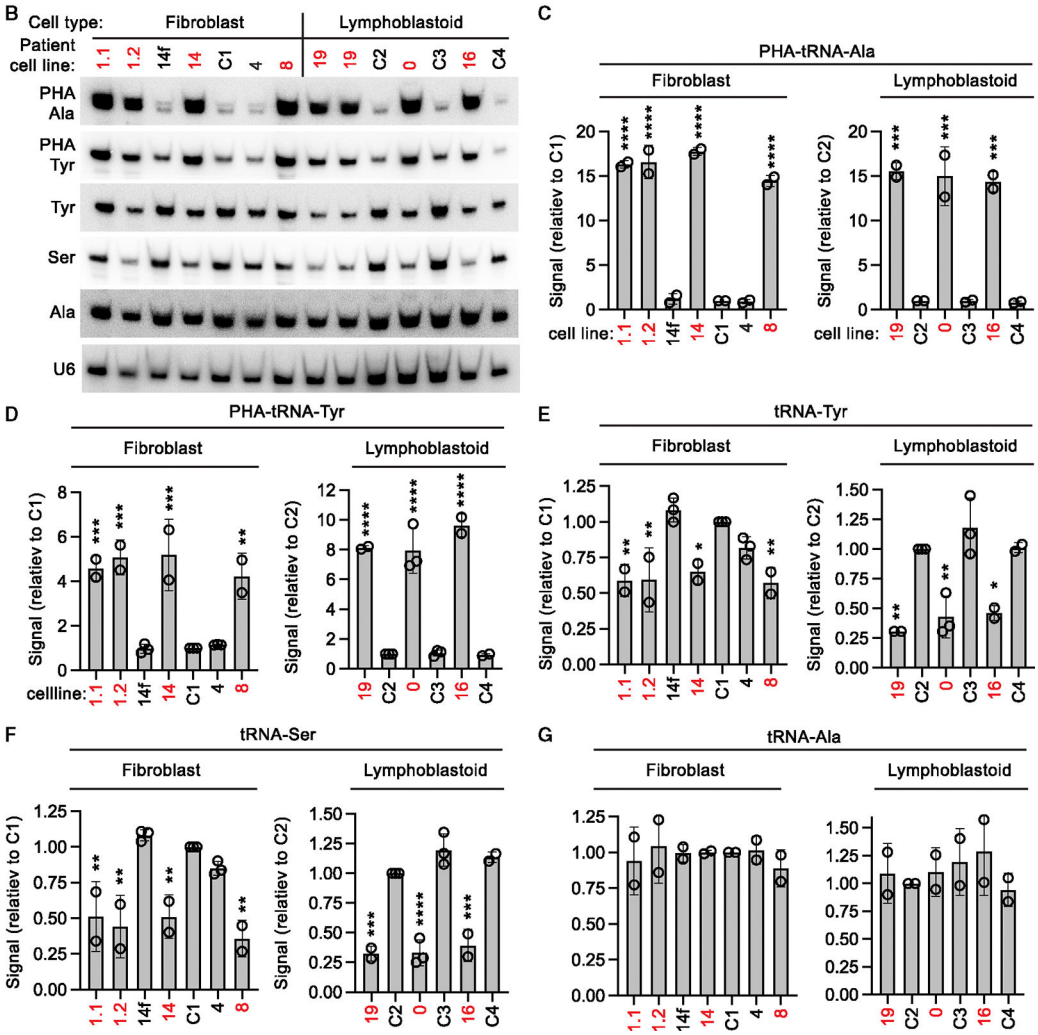

Figure 6. Human patient cells containing biallelic pathogenic TRMT1 variants exhibit a reduction in serine and tyrosine tRNA levels

(A) Patient and control cell lines used for analysis. Red indicates patients with decreased m2,2G.

(B) Northern blot analysis of cell lines derived from patient and control individuals.

(C–G) Quantification of the relative northern blot signal for the indicated tRNAs from patient cell lines versus the C1 control fibroblast cell line or C2 control lymphoblastoid cell line. Error bars indicate the standard deviation from the mean. Statistical analysis

was performed using one-way ANOVA, and significance was calculated using Dunnett's multiple comparison test. ****$p \leq 0.0001$, ***$p \leq 0.001$, **$p \leq 0.01$, *$p \leq 0.05$.

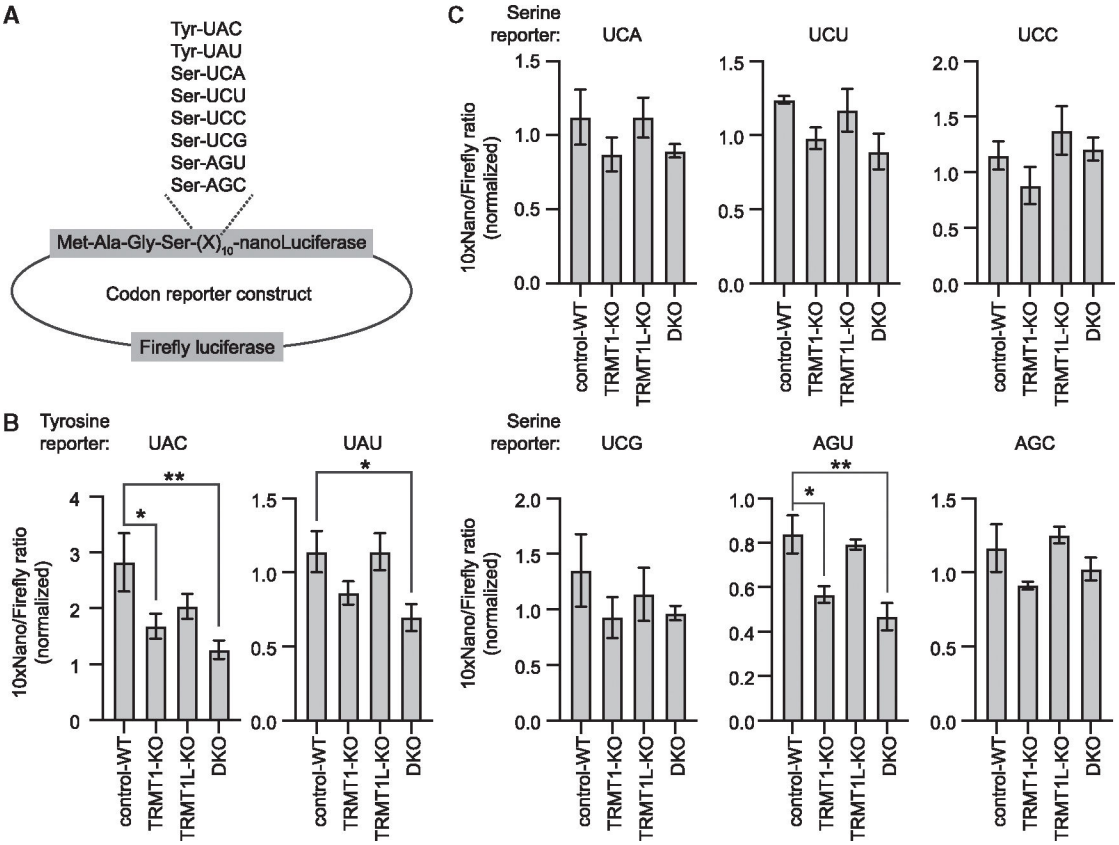

Figure 7. Loss of TRMT1 and TRMT1L impairs protein expression from specific codon reporters

(A) Codon reporter constructs.

(B) Quantification of protein expression from the tyrosine UAC and UAU codon reporters.

(C) Quantification of translation from serine codon reporters. Error bars indicate the standard error from the mean. Statistical analysis was performed using one-way ANOVA, and significance was calculated using Dunnett's multiple-comparisons test. $^{**}p \leq 0.01$, $^{*}p \leq 0.05$.

KEY RESOURCES TABLE

REAGENT or RESOURCE	SOURCE	IDENTIFIER
Antibodies		
TRMT1-G3	Santa Cruz Biotechnology	sc-373687; RRID: AB_10915423
TRMT1L	Abnova	H00081627-B01P; RRID: AB_1570771
Flag-M2	Sigma-Aldrich	F1804; RRID: AB_262044
Twin-Strep	Genscript	A01732; RRID: AB_2622218
Actin C4	EMD Millipore	MAB1501; RRID: AB_2223041
IRDye 800CW goat anti-mouse IgG	Li-Cor	926–32210; RRID: AB_621842
IRDye Goat anti-Rabbit IgG 680 RD	Li-Cor	P/*N*925–68071; RRID: AB_2721181
IRDye Goat anti-Mouse IgG 680 RD	Li-Cor	P/*N*926–68070; RRID: AB_10956588
Bacterial and virus strains		
pLenti CMV GFP Blast	Addgene	RRID: Addgene_17445
pLenti CMV GFP Puro	Addgene	RRID: Addgene_17448
NEB Stable Competent E. coli	New England Biolabs	C3040H
Chemicals, peptides, and recombinant proteins		
TRIzol LS	Invitrogen	10–296-028
ATP, [γ-32P]- 6000 Ci/mmol, 10 mCi/ml	Revvity	BLU002Z250UC
Deposited data		
Primary sequencing data deposited	Gene Expression Omnibus (GEO)	GEO: GSE263642, https://www.ncbi.nlm.nih.gov/geo/query/acc.cgi?acc=GSE263642
Experimental models: Cell lines		
Human TRMT1L variant fibroblast cell line	This paper	TRMT1L-P512L
Human TRMT1 variant fibroblast cell lines	Efthymiou et al.[30]	See reference
Human TRMT1 variant lymphoblastoid cell lines	Zhang et al.,[31] Efthymiou et al.[30]	See reference
293T human embryonic kidney cell lines	ATCC	CRL-3216; RRID: CVCL_0063
Oligonucleotides		
See Table S3	N/A	N/A
Recombinant DNA		
pX333 plasmid	Addgene	RRID: Addgene_64073
pX333-sgTRMT1	This paper	N/A

REAGENT or RESOURCE	SOURCE	IDENTIFIER
pX333-sgTRMT1L	This paper	N/A
TRMT1L cDNA plasmid	Plasmid Repository, Harvard Medical School	HsCD00337317
pcDNA3.1-TRMT1-TWIN-Strep	This paper	N/A
pcDNA3.1-TWIN-Strep-TRMT1L	This paper	N/A
pcDNA3.1–10xcodon reporters	This paper	N/A
pLenti CMV GFP Blast (659–1)	Addgene	RRID: Addgene_17445
pLenti CMV GFP Puro (658–5)	Addgene	RRID: Addgene_17448
pLenti CMV Blast TRMT1	This paper	N/A
pLenti CMV Puro TRMT1L	This paper	N/A
Software and algorithms		
GraphPad Prism	Dotmatics software company	https://www.graphpad.com
Cutadapt, v1.18	Martin[67]	https://cutadapt.readthedocs.io/en/v1.18/#
tRAX	Holmes et al.[68]	https://trna.ucsc.edu/tRAX/
Bowtie2	Langmead and Salzberg,[69] Langmead et al.[70]	https://bowtie-bio.sourceforge.net/bowtie2/index.shtml
DESeq2	Love et al.[71]	https://bioconductor.org/packages/DESeq2/
ImageJ (Fiji)	Schindelin et al.[72]	https://imagej.net/software/fiji/
Custom code	10.5281/zenodo.14223915	https://zenodo.org/records/14223915